ISTC Reports

Illinois Sustainable Technology Center

Source Apportionment of Polycyclic Aromatic Hydrocarbons in Illinois River Sediment

Kelly J. Granberg
Karl J. Rockne
University of Illinois at Chicago

ILLINOIS SUSTAINABLE TECHNOLOGY CENTER
PRAIRIE RESEARCH INSTITUTE

TR-058
June 2015
www.istc.illinois.edu

TR-058

Source Apportionment of Polycyclic Aromatic Hydrocarbons in Illinois River Sediment

Kelly J. Granberg
Karl J. Rockne
University of Illinois at Chicago

June 2015

Submitted to the
Illinois Sustainable Technology Center
Prairie Research Institute
University of Illinois at Urbana-Champaign
www.istc.illinois.edu

The report is available on-line at:
http://www.istc.illinois.edu/info/library_docs/TR/TR058.pdf

Printed by the Authority of the State of Illinois
Bruce Rauner, Governor

ACKNOWLEDGEMENTS

This research was funded by the Illinois Sustainable Technology Center (ISTC), a division of the Prairie Research Institute at the University of Illinois at Urbana-Champaign (Grant no. HWR10219). Special thanks to Dr. John C. Marlin (ISTC) for supplying all project data and providing insightful review of results. We thank Dr. Erik R. Christensen (Dept. of Civil Engineering and Mechanics, University of Wisconsin-Milwaukee) for guidance on use of source apportionment methods.

TABLE OF CONTENTS

LIST OF TABLES

LIST OF FIGURES

LIST OF ABBREVIATIONS

Ace ..... Acenaphthene
Acy ..... Acenaphthylene
Ant ..... Anthracene
BaA ..... Benzo(a)anthracene
BaP ..... Benzo(a)pyrene
BbF ..... Benzo(b)fluoranthene
BF ..... Benzofluoranthene
BghiP ..... Benzo(ghi)perylene
BkF ..... Benzo(k)fluoranthene
Chr ..... Chrysene
CL ..... Confidence Level
CMB ..... Chemical Mass Balance
COD ..... Coefficient of Determination
CT ..... Coal Tar
DahA ..... Dibenz(a,h)anthracene
DL ..... Detection Limit
EM ..... Error Model
Fla ..... Fluoranthene
Flo ..... Fluorene
HN ..... Henry
HV ..... High Volatile
ISTC ..... Illinois Sustainable Technology Center
Ind ..... Indeno(1,2,3-cd)pyrene
ISWS ..... Illinois State Water
LC ..... Lacon
LCL ..... Lower Confidence Level
LP ..... Lower Peoria
LV ..... Low Volatile
MDL ..... Method Detection Limit
MV ..... Medium Volatile
MWRD-GC ..... Metropolitan Water Reclamation District of Greater Chicago
Nap ..... Naphthalene
NIST ..... National Institute of Standards and Technology
PAHs ..... Polycyclic Aromatic Hydrocarbons
Pha ..... Phenanthrene
PMF ..... Positive Matrix Factorization
Pyr ..... Pyrene
RE ..... Relative Error
RL ..... Reporting Limit
SA ..... Source Apportionment
SRM ..... Standard Reference Material
TACO ..... Tiered Approach to Corrective Action Objectives
UP ..... Upper Peoria
USEPA ..... United States Environmental Protection Agency

ABSTRACT

The accumulation of over six million metric tons of sediment annually in the Illinois River Valley degrades its recreational, commercial, and ecological value. This necessitates dredging a large volume of sediment to restore water depth and makes beneficial reuse of the sediment a priority. Unfortunately, many reuse applications are limited by contamination from polycyclic aromatic hydrocarbons (PAHs), particularly benzo(a)pyrene in the sediments. Existing contaminant standards do not consider whether the sources of PAHs are from current petroleum combustion-based inputs or whether they represent "legacy pollution" such as coal dust released from barges, trucks, and storage. The latter is typically found in black carbon form that might be less bioavailable, and thus may not represent as high a risk for beneficial reuse. A source apportionment (SA) analysis was undertaken to identify the sources of PAHs to the Illinois River and to determine if they come from these potentially low bioavailable forms.

Priority PAHs were analyzed in 80 sediment cores sampled from Illinois River pools and backwater lakes between Hennepin, Illinois and the Peoria Lock and Dam. PAH diagnostic ratio analysis and a Positive Matrix Factorization (PMF) multivariate receptor model were used to characterize the PAH dataset, identify specific sources of pollutants, and quantify source contributions to the river sediment. Predicted sources from the SA analysis were identified using a database of compiled reference PAH profiles for coal dust, coal tar sealcoat, motor oils, biosolids, as well as fossil fuel combustion residues from gasoline and diesel engines, power plants, and coke production.

Three sources (S1, S2, and S3) were required to reconstruct most of the variation in the Illinois River contaminant dataset by PMF source apportionment. PMF results suggested that a mixed upland source and coal-derived sources including coal tar sealcoat (S1 and S2, 75%) were major contributors to sediment PAHs in the Illinois River, as well as a diffuse traffic-based source (S3, 25%). Liquid petroleum was not identified as a signficant source of PAHs to Illinois River sediment. Coal dust was not uniquely resolved from the coal-derived sources and thus could not be assessed for reduced PAH bioavailability. Finally, comparison of PMF results with those from the widely-used PAH diagnostic ratio method indicated that the latter does a relatively poor job of uniquely resolving PAH sources in the sediments.

INTRODUCTION

The Illinois River connects the Des Plaines River and the Kankakee River in northeast Illinois, USA, to the Mississippi River, draining the largest watershed in Illinois. The drainage basin is approximately 83,000 km^2 and includes metropolitan areas like Chicago (metropolitan population over eight million) but is largely (80%) agricultural. Over six million metric tons of sediment are deposited in the river valley each year from tributaries, the mainline, and bluff erosion.[1] Sedimentation has especially degraded ecological and habitat functions of river pools and backwater lakes, and severely limited recreational and commercial fishing and boating.[2] Recognizing that deposited sediments can be similar to high quality topsoil, sediment reuse advocates have called for the use of dredged material for amending restoration and reclamation sites. However, legacy sediment contaminants such as polycyclic aromatic hydrocarbons (PAHs) must be at protective levels for any beneficial use of sediment. PAHs are the most prevalent hydrophobic organic contaminant in sediments, and compose significant fractions of coal, crude oil and distillates, and combustion residues (char, soot, and other black carbon forms) of fossil and organic fuels.[3]

The Illinois Sustainable Technology Center (ISTC) and other state agencies have supported the sampling and testing of Illinois River sediment for beneficial reuse projects over the past decade.[2, 4, 5] In some cores, PAHs were measured at levels higher than state TACO (Tiered Approach to Corrective Action Objectives, Illinois Adm. Code, 2007) cleanup standards.[6] While Illinois does not have a standard for contaminants in topsoil, state TACO cleanup standards are sometimes used as a surrogate (Table 1). However from a risk standpoint, PAH bioavailability is a more important indicator of toxicity than concentration levels alone.[7] While bioavailability is difficult to measure directly, an understanding of its potential effects can be inferred by PAH source information. For example, PAHs preferentially partition to condensed black carbon forms like coal dusts and large combustion particles, where they are less likely to be bioavailable than PAHs derived from direct petroleum spills and releases.[8] It has been hypothesized that coal from stockpiles and transportation by barge over the past century may have heavily contributed to the sediment PAH burden. This hypothesis is supported in part by an elemental analysis of dried and combusted Upper and Lower Peoria Lake surface sediments sampled by the Illinois State Geological Survey. Our laboratory found that approximately 1.5% of the solids and nearly half of total carbon in the sediment exist as black or condensed carbon (Figure 1). To test this hypothesis, a source apportionment (SA) analysis was undertaken using diagnostic PAH ratios and Positive Matrix Factorization (PMF) receptor modeling to determine whether coal-based pollution was likely to have contributed to PAHs in the Illinois River. A second objective of this study was to critically compare diagnostic ratio analysis with PMF modeling for SA of priority PAHs in sediment.

Table 1. PAH background soil concentrations for populated areas and soil remediation concentration objectives (µg/kg) from TACO.[a]

	Background			
	City of Chicago	Other Metropolitan Area	Non-Metropolitan Areas	Remediation Objectives[b]
Nap	40	200	170	1.60E+06
Acy	30	70	40	na
Ace	90	130	40	4.70E+06
Flo	100	180	40	3.10E+06
Pha	1300	2500	990	na
Ant	250	400	140	2.30E+07
Fla	2700	4100	1800	3.10E+06
Pyr	1900	3000	1200	2.30E+06
BaA	1100	1800	720	900[c]
Chr	1200	2700	1100	8.80E+04
BbF	1500	2100	700	900[c]
BkF	990	1700	630	9.00E+03
BaP	1300	2100	980	90[c]
DahA	200	420	150	90[c]
Ind	860	1600	510	900[c]
BghiP	680	1700	840	na

[a] Tiered Approach to Corrective Action Objectives (TACO), Illinois Adm. Code, 2007.
[b] Based on human health criteria and ingestion exposure route. Unavailable data labeled na.
[c] For PAHs in which remediation standards are exceeded by background concentrations, background concentrations can be used instead (TACO).

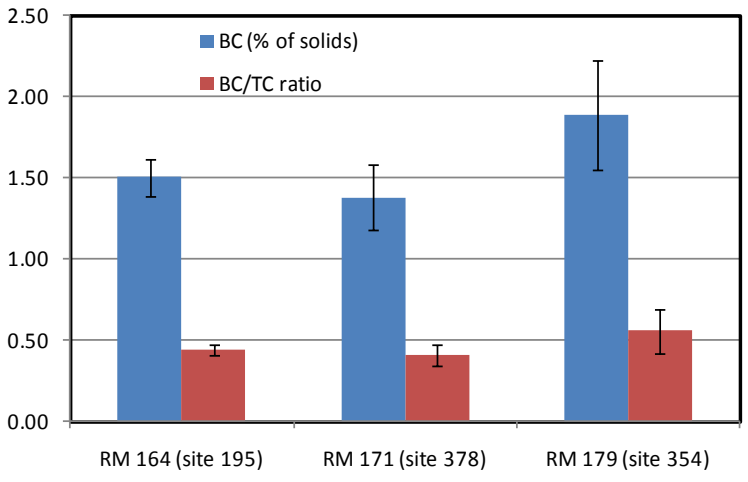

Figure 1. Black carbon in Lake Peoria sediment. Error bars indicate standard deviations for 10 cm sections.

METHODS

Sediment sampling and PAH analysis. Over 100 segmented sediment cores were collected by the Illinois State Water Survey (ISWS) between 2004 and 2007 from the central 200 km of the Illinois River and backwaters using a vibra-coring system.[5] Sediment cores were taken to an average depth of 203 cm and were segmented into evenly spaced 2 cm intervals. Composites were developed by thoroughly mixing material from the intervals for the entire length of the core, generally 2 cm of material taken every 20 cm. Cores were composited as whole cores, upper cores, or lower cores: whole cores averaged 8 cm to 203 cm (n=62), top segments averaged 8 cm to 132 cm (n=29), and bottom segments averaged 143 cm to 217 cm (n=10).

Sediment cores were analyzed for a suite of contaminants by a USEPA certified laboratory utilizing USEPA standard method 8270C.[5] Measured contaminants included the 16 EPA priority PAHs: naphthalene (Nap), acenaphthylene (Acy), acenaphthene (Ace), fluorene (Flo), phenanthrene (Pha), fluoranthene (Fla), pyrene (Pyr), benzo(a)anthracene (BaA), chrysene (Chr), benzo(b)fluoranthene (BbF), benzo(k)fluoranthene (BkF), benzo(a)pyrene (BaP), dibenz(a,h)anthracene (DahA), indeno(1,2,3-cd)pyrene (Ind), and benzo(ghi)perylene (BghiP). PAH concentrations were reported in µg/kg dry weight of sediment. Sample-specific reporting limits (RLs) varied from 20 to 330 µg/kg. Approximate concentrations were reported for measurements between the method detection limit (MDL) and the RL, and measurements below the MDL were reported as non-detect. Note dating information was not available for the cores.
The present study focused on four reaches between Hennepin, Illinois and the Peoria Lock and Dam (Figure 2) because of the high number of non-detects (40-100%) in samples downstream of the dam (n=8). Core locations are given in Figures 3 through 6 for the four study reaches named according to proximate river city and ordered from upstream to downstream: Henry (HN), Lacon (LC), Upper Peoria (UP), and Lower Peoria (LP).

While dating information and specific sedimentation rates for these cores are unknown, Cahill et al. (2008)[4] reported sedimentation rates averaged between 1 to 2 cm/yr since 1954 as determined by ^{137}Cs dating for many of the same Illinois River backwater lakes. Previous studies referencing bathymetric surveys of Upper and Lower Peoria Lakes estimated sedimentation rates between 2 and 3 cm/yr from 1903-1985 and > 5 cm/yr between 1976 and 1985, with overall rates at Upper Peoria Lake (UP) 1.5 times higher than Lower Peoria Lake (LP).[9] Although reported sedimentation rates vary over time and space, it is likely that most/all whole cores (average depth 203 cm) span the twentieth century and witnessed major anthropogenic changes to the river. These include diversion of water from Lake Michigan, construction of navigational dams, locks, and major dredging operations, as well as changes to the drainage basin such as enlargement for the Chicago metropolitan region and dramatic increases in agricultural use and intensity.[9]

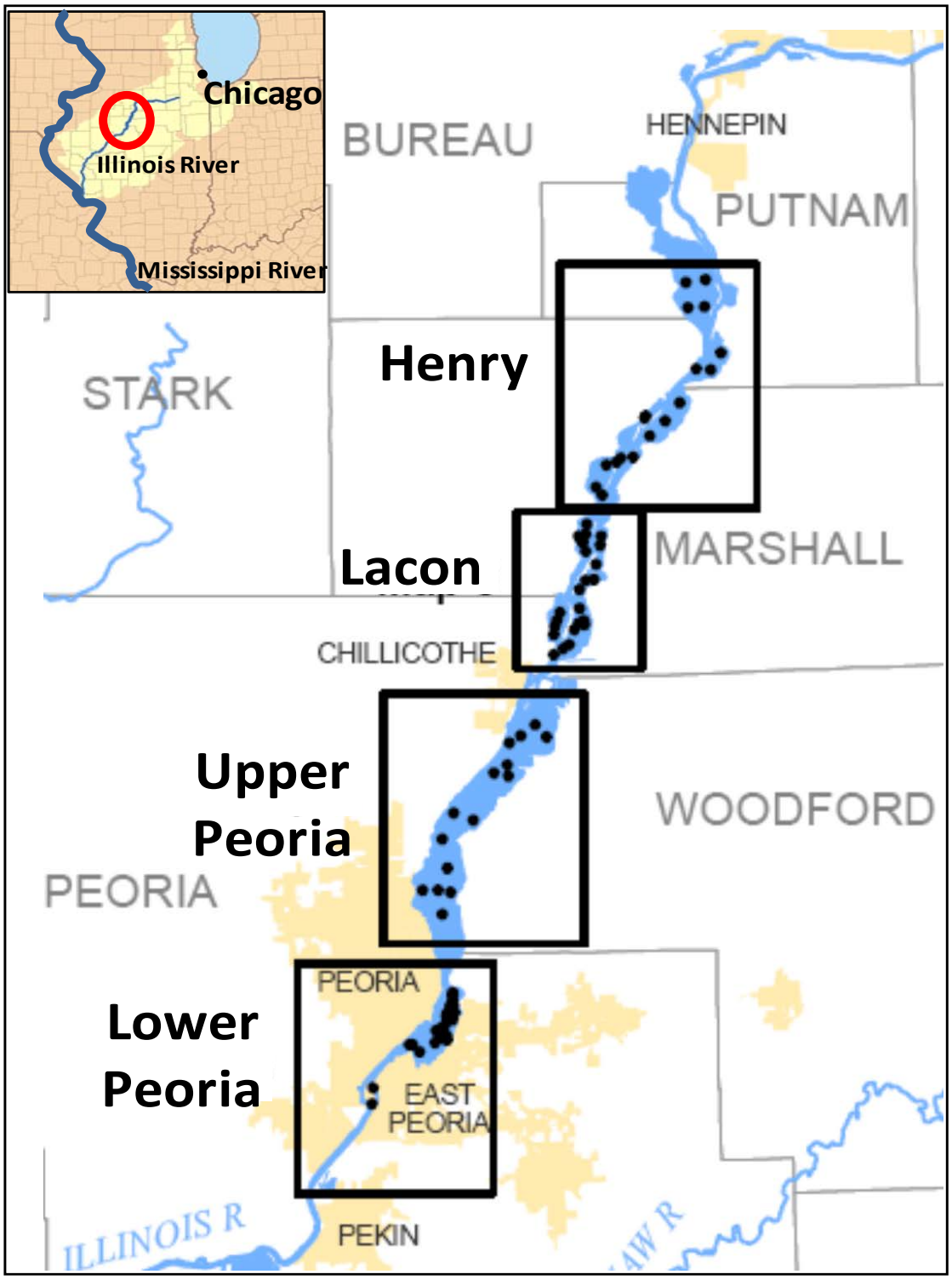

Figure 2. Map of Illinois River study location and sediment core sites. Study area is circled on the locator map (upper left) with the watershed and relationship to Chicago/Lake Michigan (upstream) and Mississippi River (downstream) shown. Cores are points and reaches are labeled (from upstream to downstream) Henry, Lacon, Upper Peoria, and Lower Peoria (see Figures 3 to 6). Counties and municipalities are also shown. Map from the ISWS (2008).[5]

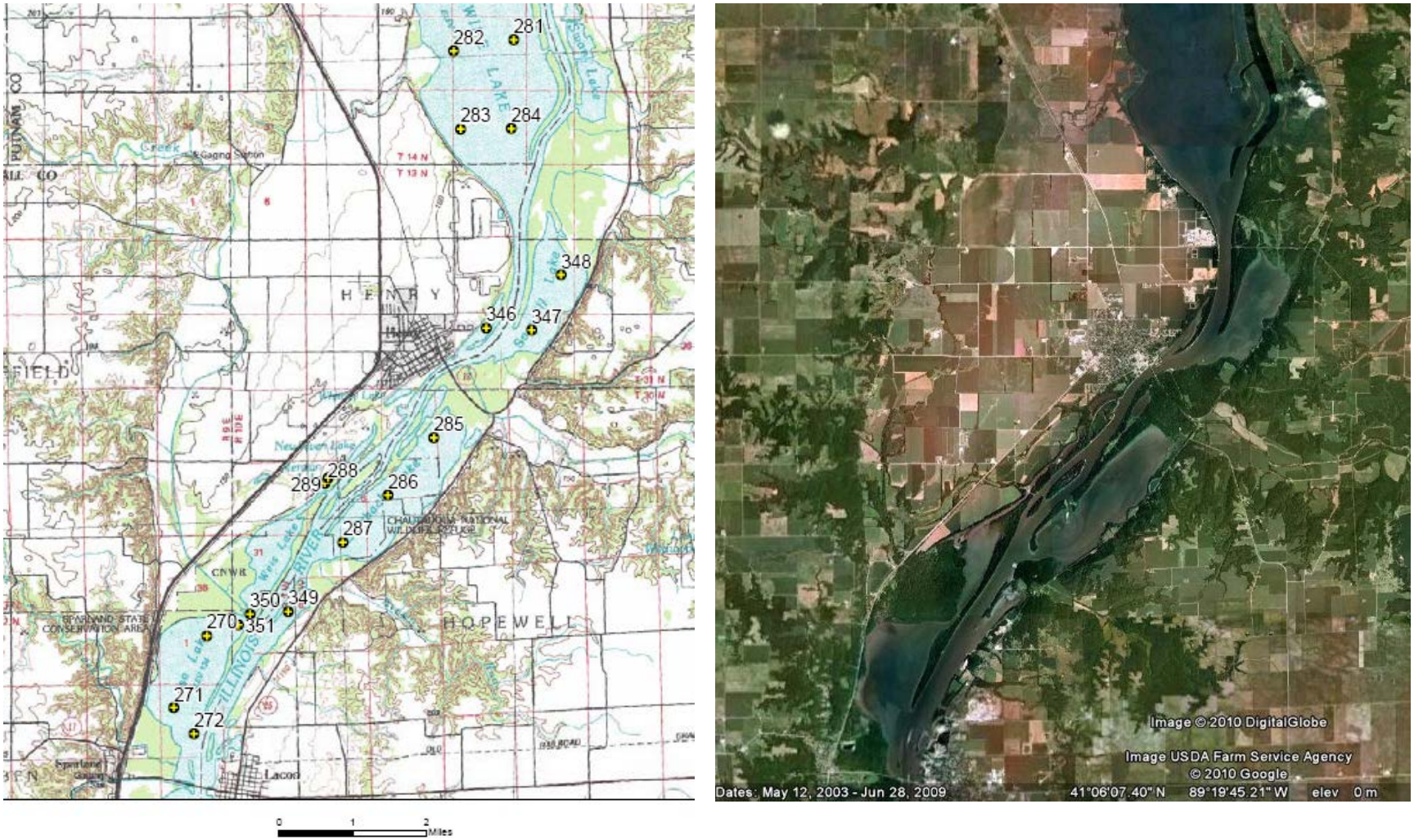

A) **B)**

Figure 3. Henry (HN) sample site on the Illinois River (includes Senachwine, Sawmill, Billsbach, Weis, and Goose Lakes). Sediment core numbers and locations shown on ISWS (2008)[5] quadrangle map (A) alongside an aerial photograph (B). Satellite photo ©Google Inc. 2008.

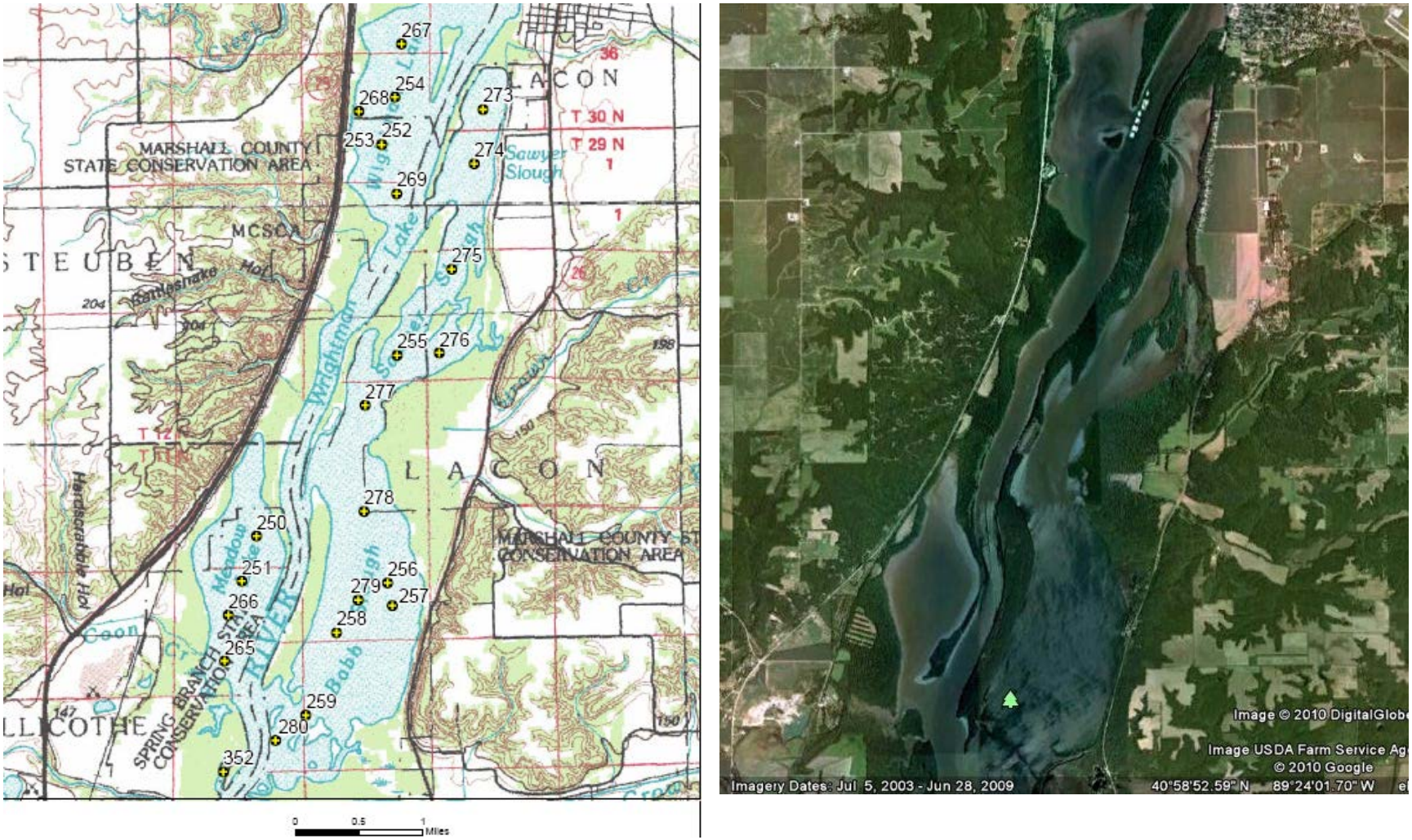

A) **B)**

Figure 4. Lacon (LC) sample sites on the Illinois River (includes Wightman Lake, Sawyer Slough, Meadow Lake, and Babb Slough). Sediment core numbers and locations shown on ISWS (2008)[5] quadrangle map (A) alongside an aerial photograph (B). Satellite photo ©Google Inc. 2008.

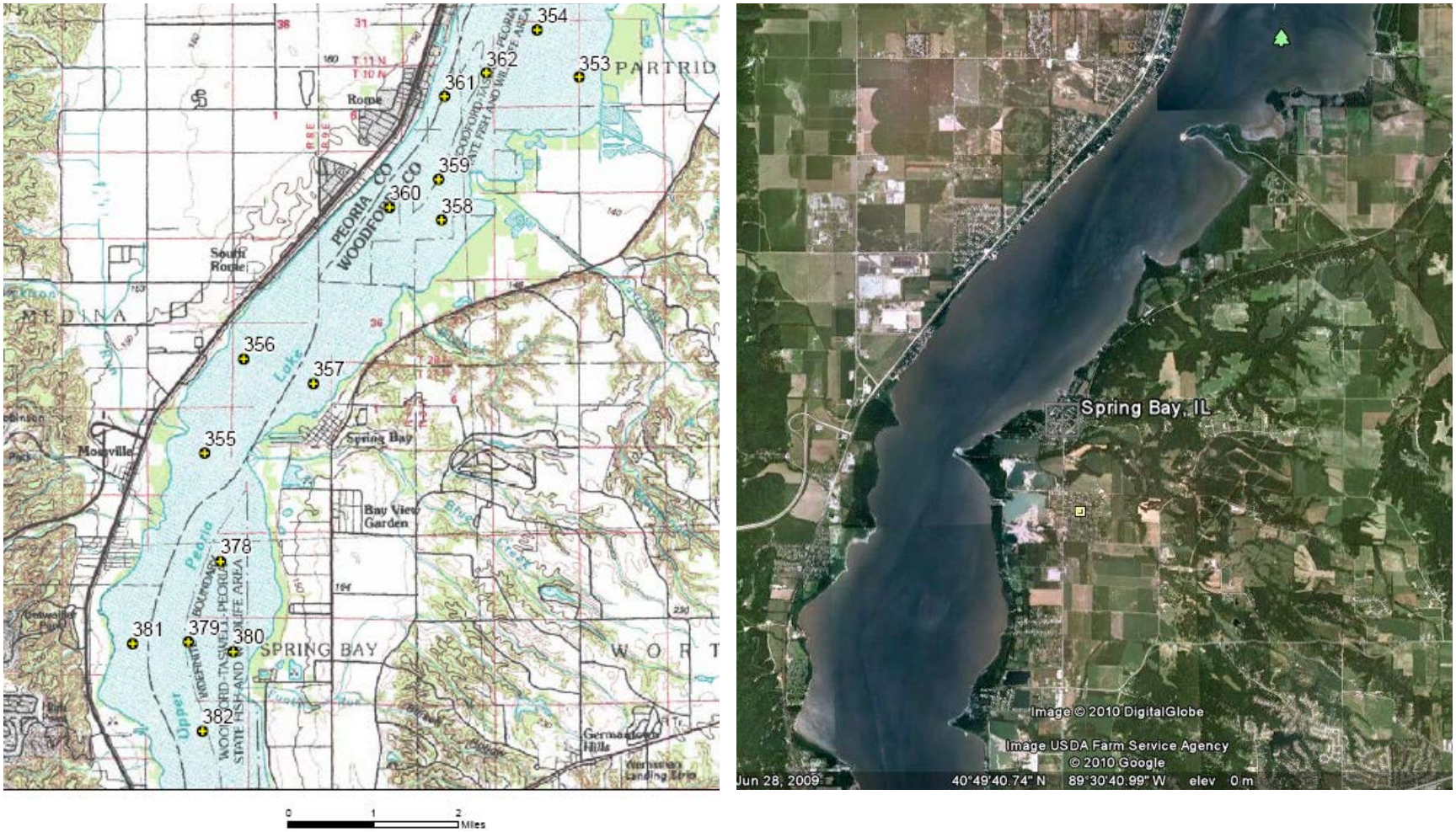

A) **B)**

Figure 5. Upper Peoria (UP) sample sites on the Illinois River (Upper Peoria Lake). Sediment core numbers and locations shown on ISWS (2008)[5] quadrangle map (A) alongside an aerial photograph (B). Satellite photo ©Google Inc. 2008.

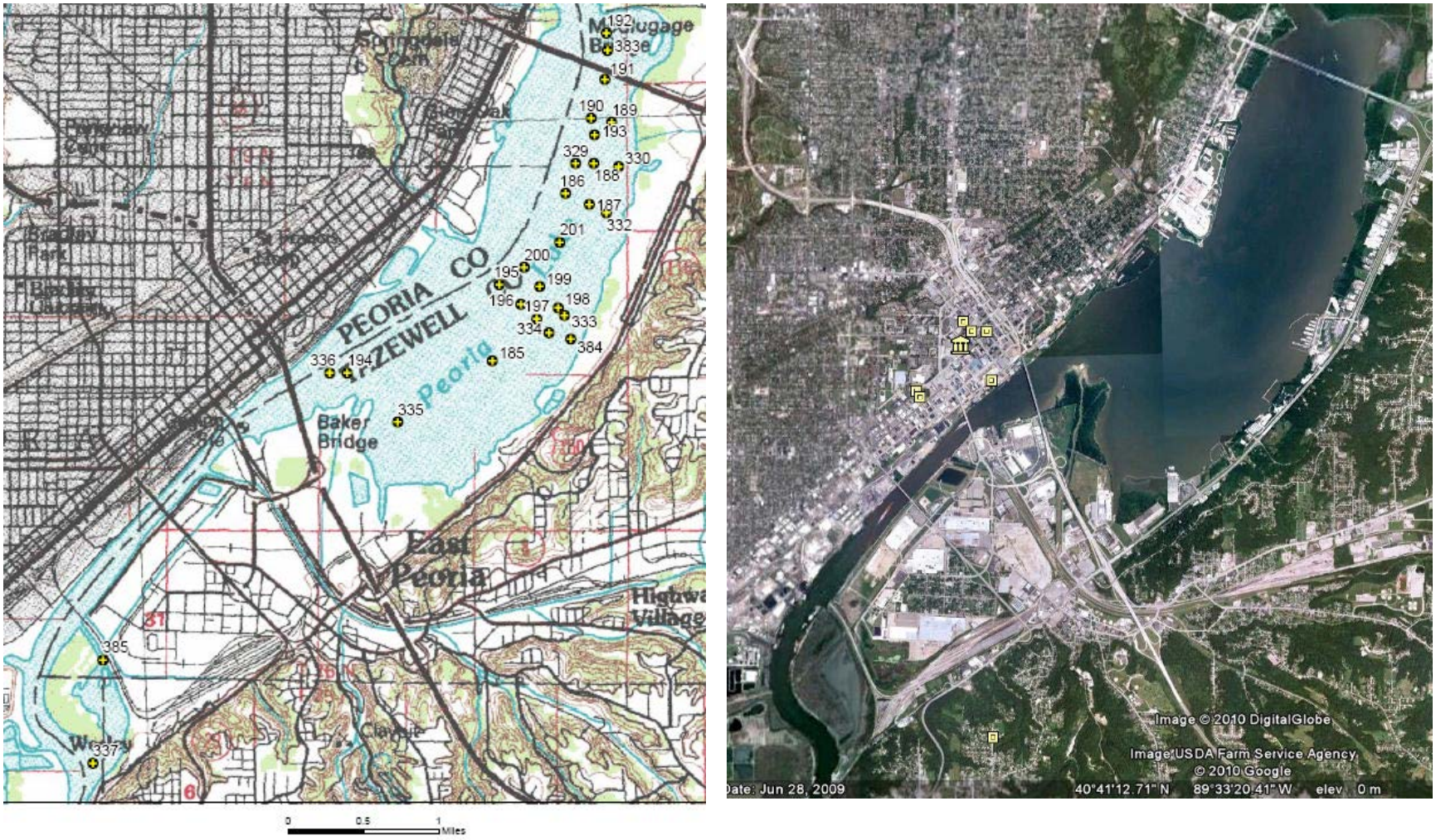

A) **B)**

Figure 6. Lower Peoria (LP) sample sites on the Illinois River (Lower Peoria Lake). Sediment core numbers and locations shown on ISWS (2008)[5] quadrangle map (A) alongside an aerial photograph (B). Satellite photo ©Google Inc. 2008.

Dataset preparation. A well-conditioned dataset retaining maximum informative capacity was prepared for source apportionment analysis. All samples were included except for cores over 40% non-detect (n=8, mainly bottom segments) and all priority PAHs were retained except for Nap and Ace which were detected only 16% and 52% of the time, respectively. All other PAHs had detection frequencies over 70%. Remaining non-detects (5% of the dataset) were replaced with half of the lowest measured analyte for each sample which was assumed to be near the true MDL. This process provided significantly more variation to the dataset than simply using the lowest measured sample value for each analyte. A linear regression analysis of ordered original and natural logarithm-transformed PAH data revealed two outliers with Studentized T-residuals > 3.0 for all original and many transformed PAHs, which were subsequently eliminated. The final PAH dataset is shown in Table 2 and comprises 14 compounds and 80 sediment cores for a total of 1120 data points.

Table 2. Illinois River sediment PAH data (µg/kg) for source apportionment analysis.[a]

Core[b]	Depth[c] (cm)	RL[d]	Acy	Flo	Pha	Ant	Fla	Pyr	BaA	Chr	BbF	BkF	BaP	DahA	Ind	BghiP
HN281	8 - 190	29	47	**24**	78	63	290	360	190	320	200	220	250	73	160	200
HN282	8 - 250	37	41	39	120	70	340	400	210	320	210	200	210	**27**	150	190
HN283	8 - 250	37	56	***18.5***	100	76	410	470	260	360	240	240	260	70	140	200
HN284t	8 - 110	35	95	45	120	84	480	510	310	480	350	250	340	110	200	260
HN346	8 - 150	65	170	**42**	240	190	1100	1400	950	1000	1000	490	990	150	380	470
HN347	8 - 170	75	81	**40**	210	140	990	1100	570	670	650	290	530	**68**	200	250
HN348	8 - 150	70	**47**	**28**	110	**70**	530	560	300	390	350	210	300	**51**	150	190
HN285t	8 - 110	28	95	34	130	98	400	480	290	450	300	240	330	110	210	250
HN286t	8 - 110	30	59	**27**	100	59	280	430	180	290	180	200	210	70	65	170
HN286b	128 - 210	20	***4.55***	***4.55***	***4.55***	***4.55***	**11**	**17**	**13**	**15**	**9.1**	**16**	**11**	***4.55***	**11**	**13**
HN287t	8 - 130	30	38	**22**	48	32	160	220	110	190	110	130	130	42	80	130
HN287t	8 - 130	30	**28**	**15**	65	31	190	230	100	180	110	140	150	**27**	110	110
HN289	8 - 230	33	79	45	130	100	280	470	240	390	200	260	280	62	160	200
HN349t	8 - 130	64	**49**	**36**	130	74	460	580	250	340	340	160	290	**56**	140	180
HN349b	150 - 270	330	**150**	**100**	440	**250**	1700	1900	1000	1200	1100	510	950	**170**	450	560
HN270	8 - 170	27	45	**18**	36	38	170	220	120	160	110	120	140	38	76	98
HN271	8 - 210	33	**29**	**17**	40	37	190	190	110	150	84	110	110	**30**	63	82
HN272	8 - 190	28	260	97	370	280	1700	2100	1900	790	800	660	1200	230	460	550
HN272t	10 - 132	31	340	130	420	300	1900	2300	1200	1500	730	770	1000	290	480	600
HN272b	150 - 192	24	**6.4**	**5.7**	**17**	**8.6**	51	82	49	55	42	**20**	44	**11**	**22**	29
LC267	8 - 170	24	**24**	**16**	36	31	170	290	120	160	89	170	150	50	79	99
LC267t	10 - 112	29	47	**27**	65	52	360	480	260	310	190	260	240	82	130	170
LC268	8 - 246	32	**31**	**22**	60	46	270	310	160	170	110	170	160	51	88	110
LC252	8 - 250	68	140	**68**	230	210	1100	1100	590	660	640	430	550	76	280	350
LC254	8 - 190	63	180	64	320	250	1500	1500	980	910	770	530	750	100	320	440
LC273	8 - 210	29	***5***	**17**	63	50	240	250	140	200	120	140	180	38	81	100
LC274	8 - 230	34	110	35	180	120	700	690	390	590	300	390	510	110	230	280
LC275	8 - 90	26	50	**17**	49	50	230	320	170	240	170	180	220	53	110	150

Table 2. (continued). Illinois River sediment PAH data (µg/kg) for source apportionment analysis.[a]

Core[b]	Depth[c] (cm)	RL[d]	Acy	Flo	Pha	Ant	Fla	Pyr	BaA	Chr	BbF	BkF	BaP	DahA	Ind	BghiP
LC276	8 - 250	25	***5***	***5***	**11**	**10**	38	44	28	34	26	32	35	**10**	**19**	29
LC276t	10 - 72	32	**23**	**8.3**	**29**	**19**	85	130	60	97	95	74	92	**28**	59	73
LC255	8 - 230	56	70	**33**	85	80	400	480	320	310	340	170	290	60	140	190
LC277	8 - 110	23	**9.2**	***3.75***	**11**	**7.5**	35	42	**18**	37	23	40	32	**12**	23	30
LC278	8 - 170	22	**11**	***5.5***	**14**	**12**	57	78	41	52	35	50	48	**13**	25	34
LC279	8 - 230	22	**11**	***5.5***	**11**	**8.9**	42	57	29	45	34	32	39	***5.5***	24	32
LC279t	10 - 92	27	**25**	**9.8**	32	**25**	110	170	77	110	83	110	100	34	68	84
LC256	8 - 230	62	**34**	**15**	**39**	**54**	200	230	110	160	170	83	120	**23**	73	100
LC265	8 - 170	25	28	**15**	53	33	150	230	160	170	130	150	160	55	95	130
LC266	8 - 190	30	63	**30**	100	79	400	640	310	460	300	340	420	130	210	280
LC250	8 - 170	56	96	**31**	140	99	500	590	420	400	450	140	390	70	190	230
LC251	8 - 230	66	120	66	170	140	710	840	550	560	530	330	460	71	220	280
LC280	8 - 130	27	71	29	300	160	710	640	410	480	330	300	430	110	210	240
LC352	8 - 90	51	***8.5***	***8.5***	**40**	**17**	98	130	65	81	97	**37**	93	**18**	**49**	70
UP353	8 - 90	50	***4.8***	***4.8***	**21**	**9.6**	55	85	**36**	52	73	**35**	55	**11**	**28**	**37**
UP354t	8 - 170	330	***47***	***47***	**160**	**96**	710	1200	490	610	650	**300**	520	**94**	**250**	330
UP362	8 - 170	58	120	93	350	210	1400	1900	850	1000	790	810	740	230	440	560
UP361	8 - 250	51	290	160	620	370	1900	2700	1500	1700	1600	750	1500	240	680	870
UP358	8 - 230	55	**44**	**21**	71	**51**	300	390	200	220	260	110	180	**40**	98	120
UP357	8 - 210	63	90	**60**	220	150	990	1300	590	660	690	320	540	96	260	340
UP356t	8 - 170	70	**31**	**19**	**50**	**37**	170	240	140	150	180	110	150	**33**	82	110
UP355	8 - 230	59	**52**	**25**	110	71	360	530	270	290	320	170	270	**56**	140	180
UP378	8 - 150	53	**27**	**17**	57	**31**	170	270	160	220	180	110	180	59	120	150
UP379	8 - 210	53	**33**	**29**	93	72	320	480	260	320	270	150	250	90	160	200
UP380	8 - 210	58	***9***	***9***	**32**	**18**	82	160	68	110	110	67	94	**37**	61	75
UP381	8 - 150	55	**27**	**19**	**52**	**30**	150	270	140	170	160	130	150	56	100	120
UP382	8 - 250	66	81	**60**	180	120	***17***	1000	450	670	490	430	500	160	290	340
LP383	8 - 250	56	**39**	**37**	92	**46**	370	430	230	310	200	240	210	57	130	150
LP192	8 - 230	56	**34**	**19**	74	**45**	300	390	130	240	180	130	150	**28**	77	100

Table 2. (continued). Illinois River sediment PAH data (µg/kg) for source apportionment analysis[a]

Core[b]	Depth[c] (cm)	RL[d]	Acy	Flo	Pha	Ant	Fla	Pyr	BaA	Chr	BbF	BkF	BaP	DahA	Ind	BghiP
LP191	8 - 190	55	**25**	**14**	78	**43**	210	320	130	200	180	110	140	**26**	78	95
LP190	8 - 230	49	**48**	**33**	95	**47**	220	400	160	280	220	150	200	**34**	110	150
LP189	8 - 250	47	**42**	**17**	100	64	350	450	160	280	220	160	180	**34**	110	130
LP329	8 - 250	69	**47**	**23**	70	**42**	270	340	170	260	200	350	250	94	200	250
LP330	8 - 110	58	***7***	***7***	**40**	**14**	97	130	**50**	60	**55**	79	68	***7***	**42**	**54**
LP186	8 - 250	49	**39**	**26**	120	58	220	460	200	250	260	170	220	**44**	130	170
LP187	8 - 190	52	**39**	**20**	91	59	290	490	160	280	210	160	190	**38**	97	120
LP188	8 - 210	50	**12**	***6***	**24**	**12**	60	110	54	62	68	53	58	**12**	**37**	**47**
LP332t	8 - 90	59	***8.5***	***8.5***	**24**	**17**	130	160	61	85	92	110	76	**27**	**59**	72
LP200	8 - 250	66	78	***33***	160	88	410	610	250	430	460	210	340	84	190	310
LP199	8 - 250	62	**47**	***21***	110	74	380	540	220	360	380	170	250	**42**	140	230
LP198	8 - 150	82	***21.5***	***21.5***	***21.5***	***21.5***	100	170	**63**	99	120	**63**	**62**	***21.5***	**43**	92
LP197t	8 - 90	63	**49**	***22.5***	100	68	360	520	200	340	350	130	240	**45**	130	220
LP196	8 - 190	60	**39**	***17.5***	84	**54**	300	430	170	260	270	140	200	**35**	120	190
LP195	8 - 250	62	69	**45**	150	82	390	650	230	390	330	210	320	**40**	190	290
LP333	8 - 150	84	***9.5***	***9.5***	**34**	**19**	85	140	**52**	**53**	**72**	**52**	**60**	***9.5***	**38**	**54**
LP384	8 - 170	94	***9.5***	***9.5***	**52**	**19**	150	170	100	120	110	150	110	**33**	**87**	110
LP335t	8 - 130	69	**22**	***11***	**56**	**42**	240	280	120	170	170	180	150	**45**	94	130
LP335b	148 - 230	73	**21**	***10.5***	**47**	**23**	150	190	92	110	130	120	130	***10.5***	89	110
LP336	8 - 190	48	***7***	**14**	99	**24**	210	200	83	130	120	110	120	**34**	82	100
LP194	8 - 230	45	***15***	***15***	75	***15***	110	120	53	71	81	**36**	49	***15***	**30**	57
LP385	8 - 230	44	**14**	**31**	110	***7***	180	210	110	160	100	110	94	**19**	72	84
LP337	8 - 250	47	**29**	81	420	130	670	550	310	370	260	280	320	77	170	190

[a] 14 PAHs and 80 samples. Bold values indicate approximate concentrations measured between the Method Detection Limit (MDL) and Reporting Limit (RL); italicized values indicate non-detect substitution with half the lowest analyte measurement (or RL in few cases where it is lower) for the sample.

[b] Ordered generally from upstream to downstream. Naming convention by river reach (HN, LC, UP, LP), location number (186-385 corresponding to Figures 3-6), and whether whole core composite (no suffix) or segment composite (t denotes top, b denotes bottom).

[c] Given as Upper Core Depth – Lower Core Depth.

[d] Reporting Limit (RL) in µg/kg.

PAH Diagnostic Ratios. Diagnostic ratios have been developed to identify PAH sources in the environment based on relative characteristic proportions of PAHs in basic source types[10-15] and are extensively used in environmental forensics studies (e.g., Yunker et al. (2002)[10] has been cited in excess of 1100 times as of June, 2013). Diagnostic ratios consist of PAHs with stability ranges that represent thermodynamic (fossil) versus kinetic (combustion) formation and distinguish between sources based on relative proportions of one PAH to the other. Ratios typically contain PAHs of a given molecular mass such as 178 (which includes Ant and Pha) and 202 (which includes Fla and Pyr) to minimize complications from varying PAH properties.[10]

Yunker et al. (2002)[10] reviewed four parent PAH diagnostic ratios Ant/178, Fla/Fla+Pyr, BaA/228, and Ind/Ind+BghiP for determining PAH sources in sediment and has reported ratio ranges indicating fossil versus combustion sources as well as values for a number of petroleum-derived, combustion-derived, and environmental samples (Table 3).[10, 15] Some ratios further distinguish liquid (petroleum) fuel combustion from solid (biomass/coal) fuel combustion. Although coal is not clearly differentiated from petroleum fossil fuel, ranges from samples have been reported.[15] Molecular weight 178 refers to Ant+Pha and molecular weight 228 refers to BaA+Chr+Triphenylene (note however that the latter PAH is not considered in the present study).

Diagnostic PAH ratios were calculated for measured PAHs in Illinois River sediment and compared with diagnostic source ranges (Table 3) for identification in ratio scatter plots. A second diagnostic ratio analysis was performed on the Illinois River dataset following Positive Matrix Factorization (PMF) modeling (described in the next section). PAH ratios of both the PMF-modeled sources and reference sources were compared in diagnostic ratio scatter plots to provide another approach to source identification and a comparison of both methods.

Table 3. PAH diagnostic ratios of petroleum and combustion sources and samples.[a] Diagnostic ranges are bold.

	Ant/ 178	Fla/ Fla+Pyr	BaA/ 228	Ind/ Ind+BghiP
Petroleum	**< 0.1**	**< 0.4**	**< 0.2**	**< 0.2 (< 0.1)[b]**
Kerosene	0.04	0.46	0.35	0.48
Diesel oil (n=8)	0.09	0.26	0.35	0.4
Crude oil (n=9)	0.07	0.22	0.12	0.09
Australian crude oils and fluid	0.03	0.43		
Shale oil	0.26	0.34	0.45	0.39
Lubricating oil		0.29	0.1	0.12
Coal (n=27)	0.2			
Asphalt			0.5	0.53
Coal (n=2)[c]	0.03 - 0.07	0.36 - 0.37	0.37 - 0.40	0.14 - 0.16
Combustion				
Liquid/Petroleum Fossil Fuel	**> 0.1**	**0.4 - 0.5**	**> 0.35**	**0.2 - 0.5 (0.1 - 0.3)[b]**
Solid/Grass/Wood/Coal	**> 0.1**	**> 0.5**	**> 0.35**	**> 0.5 (> 0.3)[b]**
Lignite and brown coal (n=3)	0.08	0.72	0.44	0.57
Bituminous coal (n=3)	0.33	0.53	0.34	0.48
Hard coal briquettes (n=9)		0.57	0.43	0.52
Coal tar (SRM 1597)	0.18	0.58	0.54	0.53
Wood soot (n=2)	0.26	0.5	0.46	0.55
Wood (n=19)	0.19	0.51	0.46	0.64
Grasses (n=6)	0.17	0.58	0.46	0.58
Gasoline (n=2)	0.11	0.44	0.355	0.155
Kerosene (n=3)	0.14	0.5	0.37	0.37
Diesel (n=25)	0.11	0.39	0.38	0.35
No. 2 fuel oil (n=2)	0.06	0.51	0.17	
Crude oil (n=4)	0.22	0.44	0.49	0.47
Environmental Samples				
Bush fire		0.61	0.23	0.7
Savanna fire particulate (n=3)		0.59		0.39
Road dust	0.18	0.42	0.13	0.51
Lubricating oil, re-refined		0.74		0.36
Used engine oil, gasoline passenger car	0.22	0.3	0.5	0.18
Used engine oil, diesel car, truck & bus		0.37		0.29
Tunnel with light duty gasoline vehicles (n=4)		0.45	0.46	0.3
Tunnel with heavy duty diesel trucks & gasoline vehicles n=5)		0.42	0.57	0.3
Roadway tunnels (n=2)	0.13	0.43	0.42	0.3
Urban air (including SRM 1648 & 649;n=3)	0.8	0.56	0.3	0.4
Creosote treated wood piling (n=4)	0.2	0.62	0.5	0.64

[a] Reproduced from Yunker et al.(2003).[10] 178 indicates Ant+Pha and 228 indicates BaA+Chr+ Triphenylene (note only BaA and Chr are considered in the present study). Petroleum and combustion ranges used in diagnostic ratio plots are bold.
[b] Updated ranges are in parentheses, from Yunker et al. (2012).[15]
[c] Coal range from Yunker et al. (2012)[15] is based on samples of shipwrecked high volatile A bituminous coal.

Positive Matrix Factorization. A Positive Matrix Factorization (PMF) multivariate receptor model was used to quantitatively apportion measured PAH mass in Illinois River sediment to sources of contaminants. PMF has commonly been applied to particulate matter in air, but the technique has also been successfully used to apportion PAHs in sediments,[16] as have other multivariate[17, 18] and mass balance[19-22] receptor models. Multivariate receptor models assume measured concentrations are a linear sum of sources and utilize factor analysis to solve Equation 1 for *m* compounds in *n* samples as contributions from *p* independent sources.[23-25] The model assumes sources have unique contaminant compositions that change little during transport.[20, 26] In the present study, we assume sediment receives PAHs mainly in particulate-associated form, that these PAHs are relatively stable,[20] and that they come from sources relatively nearby (such as barge coal).[17]

$$\mathbf{X} = \mathbf{G} \text{ x } \mathbf{F} + \mathbf{E} \quad (1)$$

X is the measured concentration data matrix *m x n;* **G** is the factor-loading matrix *m x p*, representing chemical profiles for sources; **F** is the factor-score matrix *p x n*, representing source contributions for sample concentrations; **E** is the error concentration matrix *m x n*, or the difference between measured and calculated matrices.

PMF uses a constrained weighted least squares approach to solve Equation 1, iteratively computing **G** and **F** by minimizing an objective function Q (Equation 2). During Q minimization, **G** and **F** are constrained to non-negativity to ensure physically realistic source profiles and contributions. PMF weights measured data by their estimated uncertainties to reduce the influence of censored and outlier data on solutions.[27, 28]

$$Q(\mathbf{E}) = \sum_{i=1}^{m} \sum_{j=1}^{n} \left(\frac{\boldsymbol{E}_{ij}}{\boldsymbol{\sigma}_{ij}} \right)^2 \quad (2)$$

Q is the objective function or the weighted sum of squares difference between estimated and measured data; $\mathbf{E}_{ij}$ is the error concentration matrix; $\boldsymbol{\sigma}_{ij}$ is the standard deviation concentration matrix of uncertainties weighting each measured element.

This study utilizes the PMF program coded by Bzdusek (2005)[29] on the MATLAB platform (release 2011a, Mathworks, Inc., Natick, MA, USA). The model employs penalty terms for imposing constraints, and has been shown to obtain results similar to the standalone PMF program available from USEPA.[24, 30] Details of the algorithm can be found in Bzdusek (2005)[29] and convergence criteria, step length control, penalty coefficients, and other variable model parameters are described in Granberg (2013).[31] Input to the model includes the measured data matrix, the weighting matrix, and the number of sources. The weighting matrix is estimated by environmental error model (EM) = -14[31-33] with a relative error of 0.25 representing analytical, sampling, and environmental uncertainties.

Sensitivity analysis. In addition to the 14x80 data matrix (referred to in the text as 14x80), three other datasets were input to assess the sensitivity of the PMF model: a 14x84 dataset including the two outliers and two cores with low rates (40-50%) of PAH detection (referred to as 14x84OUT); a 15x84 dataset including the PAH Ace (referred to as 15x84); and a 14x84 dataset with non-

detects substituted with half the lowest value for each analyte rather than for each sample (referred to as 14x84ND). The PMF model was run multiple times investigating different numbers of sources. Diagnostic tools including coefficients of determination (CODs), Exner function, the objective function Q (or chi-square), and the number of degrees of freedom were also generated with each run to assist in evaluating goodness of fit between modeled and measured data and in choosing the correct solution and number of sources.[29]

Source profile analysis. The model output consists of source profiles (**G**) normalized to total source contaminant mass (in this case Σ_{14} PAHs for each source) in units of mass percent. Inspection of PMF profiles and comparison with known reference profiles are essential for identifying potential sources. The cosine phi (cos φ) coefficient of proportional similarity metric (Equation 3) was used to calculate the similarity of PMF and reference source profiles where the cosine of the angle φ between the vectors equals one if they are identical (i.e. angle φ = 0) and zero if dissimilar (i.e. perpendicular).[31, 34]

$$\cos\varphi = \frac{\sum_{i=1}^{m} x_i y_i}{\sqrt{\sum_{i=1}^{m} x_i^2}\sqrt{\sum_{i=1}^{m} y_i^2}} \quad (3)$$

x_i and y_i are model and reference concentrations, respectively, for compound *i*.

Nearly 50 coal, oil, combustion, and other urban PAH source profiles from the scientific literature were compiled, representing a variety of sources. Reference profiles were computed as a mass percent (usually of Σ_{14} PAHs) for direct comparison to model profiles. Non-detect PAHs were considered as zero or as half the detection limit (when available) for profile computation and cos φ calculations. When individual PAHs were unavailable they were not included in the cos φ calculations. Note that profiles may not add to exactly 100% because of rounding.

Select reference profiles are shown in Figure 7 and the complete set of reference profiles are tabulated and described in Tables 4 through 6. Coal profiles in Table 4 from Stout and Emsbo-Mattingly (2008)[35] include coals of various levels of diagenetic alteration such as less mature lignite and sub-bituminous 'brown' coals commonly used for power generation, bituminous coals commonly used in industrial applications like coke production for iron and steel industry, and highly mature less common anthracite.[36] Profiles of coal or coke particles recovered from marine sediments near a sunken coal carrying vessel by Victoria, BC, Canada,[37] and of coal dust used in a PAH bioavailability study[38] were also included. Combustion profiles (Table 5) include literature-compiled coal and traffic-derived profiles from Li et al. (2003)[20] and a wood burning profile from Bzdusek et al. (2004)[17] adjusted to particulate-only form using reported gas-particle partitioning in air.[20, 31] Gasoline and diesel soot,[39] diesel particulate,[40] and modern diesel equipment (adjusted from total to particulate-only profile)[41] were also included. Table 6 includes a variety of other anthropogenic, oil, and particulate PAH sources including Metropolitan Water Reclamation District of Greater Chicago (MWRD-GC) biosolids,[42] new and used lubricating oil,[43] and a number of coal tar (CT) related sources including coal tar,[44] creosote,[45] coal tar sealcoat runoff dust,[46] and coal tar sealcoat dust from Chicago suburb parking lots, driveways, and nearby streets.[47] Additional traffic-related profiles include street dust[48] and tire debris, used crankcase oil, asphalt, and roadside air (adjusted from total to particulate-only profile)[39] as well as urban dust.[49]

Source contribution analysis. Contributions from each source to the total PAH burden at each sample (**F**) are presented in concentration units (µg/kg). Source contribution plots can be examined in terms of river location (reach, lake, or main channel) and proximity to tributaries, urban runoff, and point sources to aid source identification. Though overall core depths and a few depth-resolved cores (top and bottom segments) are available, lack of sediment dating precludes the use of specific time records to inform the analysis. Physical and chemical characteristics of the sediment were not available to consider other drivers of PAH contamination.

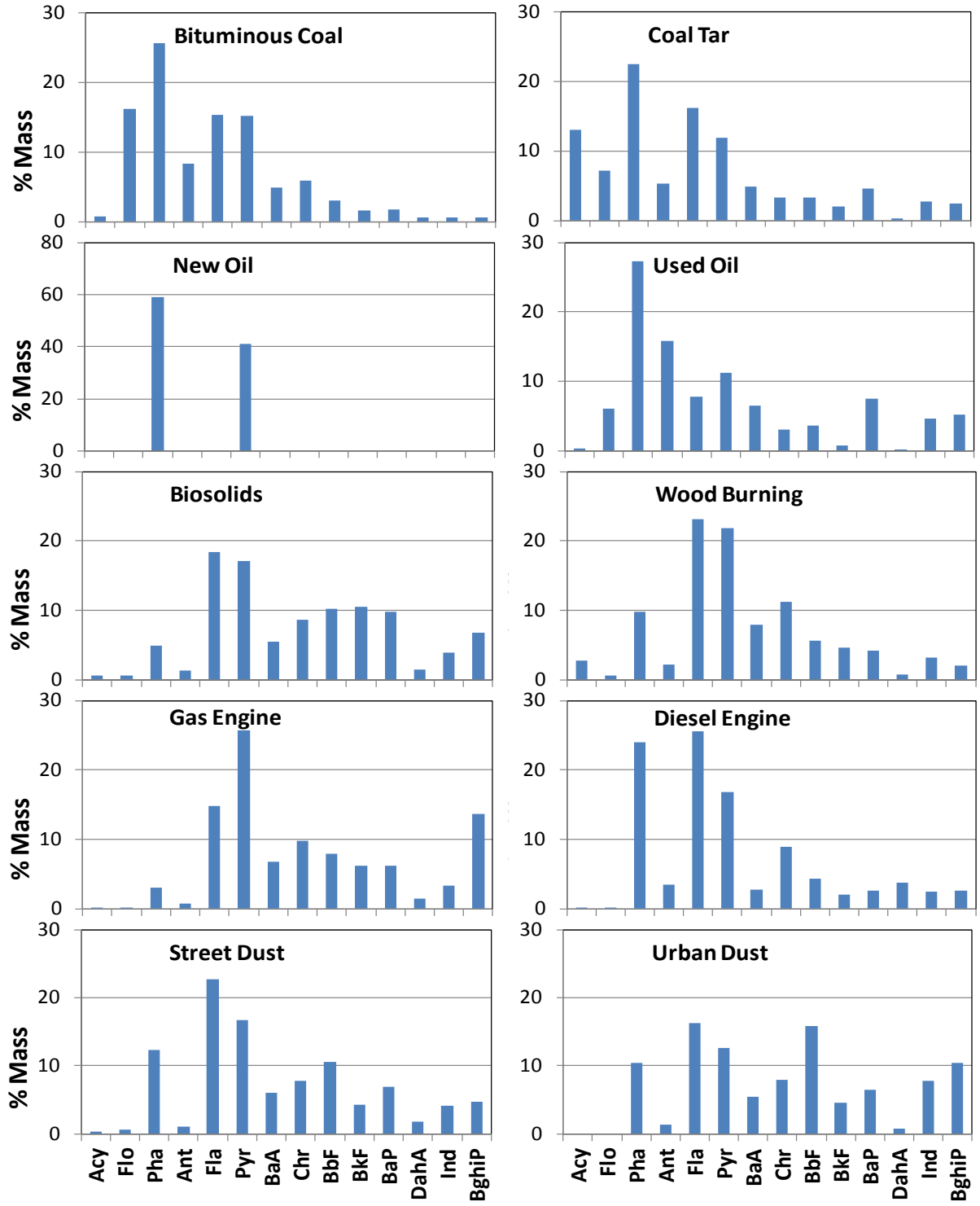

Figure 7. Select PAH reference source profiles. Bituminous coal (high-volatile C rank) from Stout and Emsbo-Mattingly (2008),[50] coal tar from Wise et al. (2010),[44] new and used lubricating oils from Wang et al. (2000),[43] biosolids an average from two MWRD drying bed samples for Gulezian et al. (2012),[42] wood burning from Bzdusek et al. (2004),[17] gas and diesel engine from Li et al. (2003),[20]street dust from Boonyatumanond et al. (2006),[48] and urban dust standard from NIST (2009).[49] Note all axes are the same except for new oil.

Table 4. Coal PAH source profiles (%).[a]

	LigA1	LigA2	SubC1	SubC2	SubB1	SubB2	SubA	HVC	HVB	HVA1	HVA2	MV	LV	Semi	Anth	Coal or coke[b]	Coal dust[c]
Acy	nd	nd	nd	nd	nd	nd	0	1	1	1	3	1	0	nd	nd	2	5
Flo	2	1	3	0	8	4	0	16	15	11	10	11	23	8	28	8	9
Pha	6	8	4	10	23	15	1	26	46	23	54	60	43	30	48	26	34
Ant	1	1	1	nd	1	1	1	8	0	18	1	1	1	0	nd	7	3
Fla	31	14	24	20	23	29	17	15	5	12	4	3	1	2	nd	8	11
Pyr	17	28	41	24	23	28	18	15	10	9	7	4	3	3	24	9	9
BaA	5	10	6	5	7	6	7	5	6	7	6	3	3	1	nd	8	2
Chr	7	10	7	14	5	6	7	6	5	9	6	13	14	20	nd	8	19
BbF	16	14	6	10	3	4	21	3	3	3	2	2	6	21	nd	7	BF 6
BkF	6	7	3	5	2	2	10	2	2	2	2	0	0	1	nd	2	
BaP	2	3	2	5	2	2	7	2	4	2	3	1	1	2	nd	7	1
DahA	1	0	0	0	0	0	1	1	0	0	0	0	1	3	nd	1	na
Ind	4	4	2	5	1	1	7	1	1	1	1	0	1	3	nd	3	na
BghiP	1	1	1	3	0	1	3	1	2	1	2	1	3	5	nd	4	1

[a] First fifteen profiles from concentrations in coals of various rank from Stout and Emsbo-Mattingly (2008):[35] Lig (Lignite) A and B; Sub (Sub-bituminous) C1, C2, C3, B1, B2, and A; Bituminous HV (High Volatile) C, B, A1, and A2; Bituminous MV (Medium Volatile); Bituminous LV (Low Volatile); Semi (semi-anthracite); and Anth (anthracite). Non-detect PAHs indicated by nd.

[b] From Chapman et al. (1996)[37] from concentrations in particles recovered from marine sediments.

[c] From Bender et al. (1987)[38] concentrations in coal dust extract..Benzofluoranthene (BF) given in place of BbF and BkF. Unavailable PAHs indicated by na.

Table 5. Combustion PAH source profiles (coal, petroleum, and wood) (%).[a]

	Coke Oven	Power Plant	Residential	Ave Coal	Gas Engine	Diesel Engine	Ave Gas & Diesel	Traffic Tunnel	Ave Petroleum	Wood Burning	Gas Soot	Diesel Soot	Diesel Particulate	Diesel Equip.
Acy	4	na	na	2	0	0	0	1	1	3	na	na	na	6
Flo	2	1	0	1	0	0	0	1	1	0	na	na	na	5
Pha	7	15	34	17	3	24	19	10	17	10	4	30	33	37
Ant	2	2	7	3	1	4	3	2	3	2	1	4	4	3
Fla	8	17	22	14	15	26	23	10	17	28	5	12	23	6
Pyr	8	15	9	12	26	17	19	12	17	26	9	20	21	19
BaA	11	10	5	9	7	3	4	6	5	8	5	5	3	3
Chr	12	20	7	12	10	9	9	10	10	9	5	11	6	5
BbF	13	8	7	10	8	4	5	9	6	3	BF 13	BF 7	3	4
BkF	8	2	3	5	6	2	3	6	4	3			1	1
BaP	10	4	3	6	6	3	3	7	5	3	11	5	1	3
DahA	2	1	na	1	2	4	3	4	3	0	na	na	0	0
Ind	4	3	2	3	3	3	3	9	6	2	15	3	2	3
BghiP	7	4	2	4	14	3	5	11	7	1	32	5	3	5

[a] Coke oven, power plant, residential, average coal, gasoline engine, diesel engine, average gas and diesel engine, traffic tunnel, and average petroleum reported by Li et al. (2003)[20] and wood burning reported by Bzdusek et al. (2004)[17] from mean of profiles compiled from the literature and corrected to particulate- only profiles from reported gas-particulate partition coefficients. Gasoline and diesel soot from Boonyatumanond et al. (2007);[39] total benzofluoranthene (BF) given in place of BbF and BkF Diesel particulate standard from National Institute of Standards and Technology (NIST) (2008).[40] Modern diesel equipment emission with catalytic control (steady state engine out test configuration) from Laroo et al. (2011)[41] was adjusted from total (gas + particulate) to particulate only profile using reported partitioning in air from Li et al. (2003).[20] Unavailable PAHs indicated by na.

Table 6. Oil, coal tar, traffic, and other particle-derived PAH source profiles (%).[a]

	Bio-solids	New Oil	Used Oil	Coal Tar (CT)	Creosote	CT Seal Dust A	CT Seal Dust B	CT Seal Parking Lot Dust	CT Seal Drvwy Dust	Street Dust by CT Lots	Street Dust	Tire Debris	Used Crankcase Oil	Asphalt	Road-side Air	Urban Dust
Acy	1 ±0	Nd	0	13	na	na	na	0 ±0	0 ±0	0 ±0	na	na	na	na	na	na
Flo	1 ±0	Nd	6	7	19	1 ±0	1 ±0	0 ±0	1 ±0	1 ±0	na	na	na	na	na	na
Pha	5 ±2	59	27	23	30	15 ±3	11 ±3	12 ±1	13 ±3	12 ±1	11	5	29	22	2	10
Ant	1 ±0	Nd	16	5	30	2 ±1	2 ±1	1 ±0	1 ±0	1 ±1	2	1	10	4	0	1
Fla	18 ±4	Nd	8	16	9	32 ±2	27 ±1	25 ±2	28 ±0	23 ±0	23	15	13	10	4	16
Pyr	17 ±4	41	11	12	5	21 ±1	21 ±1	19 ±1	20 ±1	17 ±0	25	42	21	14	7	13
BaA	6 ±1	Nd	6	5	na	6 ±2	9 ±1	5 ±1	5 ±0	6 ±1	6	2	6	3	5	6
Chr	9 ±2	Nd	3	3	5	14 ±2	16 ±1	9 ±1	8 ±1	8 ±0	11	9	5	9	12	8
BbF	10 ±1	Nd	4	3	na	na	Na	11 ±1	9 ±1	11 ±1	BF 9	BF 4	BF 4	BF 12	BF 33	16
BkF	10 ±3	Nd	1	2	na	na	Na	3 ±0	3 ±0	4 ±0						5
BaP	10 ±1	Nd	8	5	2	7 ±2	10 ±2	6 ±1	5 ±0	7 ±0	4	3	5	8	17	7
DahA	1 ±0	Nd	0	0	na	2 ±1	2 ±1	1 ±0	0 ±0	2 ±1	na	na	na	na	na	1
Ind	4 ±1	Nd	5	3	na	na	na	4 ±1	3 ±0	4 ±0	3	2	3	5	2	8
BghiP	7 ±1	Nd	5	3	na	na	na	5 ±1	4 ±0	5 ±1	7	17	4	12	17	10

[a] Biosolids from two Metropolitan Water Reclamation District-Chicago District (MWRD-CD) drying bed grab samples from Gulezian et al. (2012);[42] mean profile ± range/2. New and used lubricating oil from Wang et al. (2000);[43] non-detects indicated by nd. Coal tar (CT) standard from Wise et al. (2010).[44] Creosote from Mueller et al. (1989).[45] Coal tar (CT) sealcoat dust runoff of test plots A and B from Mahler et al. (2005);[46] mean profiles ± σ from n=3 sampling events for each. CT sealed parking lot, driveway, and nearby street dust of Chicago suburb from Van Metre et al. (2008);[47] mean profiles ± σ (parking lot, n=3), ± range/2 (driveway, n=2), and ± σ (street dust, n=3). Street dust from Boonyatumanond et al. (2006)[48] and tire debris, used crankcase oil, asphalt, and roadside air from Boonyatumanond et al. (2007);[39] benzofluoranthene (BF) given in place of BbF and BkF; roadside air is adjusted from total to particulate only profile using reported partitioning in air from Li et al. (2003).[20] Urban dust standard from National Institute of Standards and Technology (NIST) (2009).[49] Non-detect PAHs indicated by nd and unavailable PAHs indicated by na.

RESULTS AND DISCUSSION

Measured levels and trends. Mean PAH concentrations (Figure 8) from the 80 Illinois River sediment cores ranged from 25 µg/kg (Flo) to 520 µg/kg (Pyr). The mean profile was dominated by four-ring PAHs and similar in appearance to the gas engine profile (see Figure 7). Sediment PAH concentrations were less than TACO[6] background soil concentrations and cleanup standards (see Table 1) for all PAHs except for BaP (281 µg/kg relative to its remediation standard of 90 µg/kg).

Based on Lilliefors test for normality and histogram plots (Figure 9), PAHs were not normally distributed and more closely approximate a log-normal distribution. Total PAHs (Σ14 PAHs) ranged from 139 to 14880 µg/kg (Figure 10). Except for site HN349, Σ14 PAHs in bottom segments were significantly less than in top segments and whole cores. This suggests that PAH contamination was lower in the past. While no clear trend is evident from upstream to downstream, Σ14 PAHs levels were typically elevated in sediments near the main channel (HN 346-347, HN 272, LC 252-254, UP 361-362). PAH levels were also lower and less variable in reach LP (Figure 10). UP and LP were the only reaches with significantly different ($p < 0.05$) PAH levels.

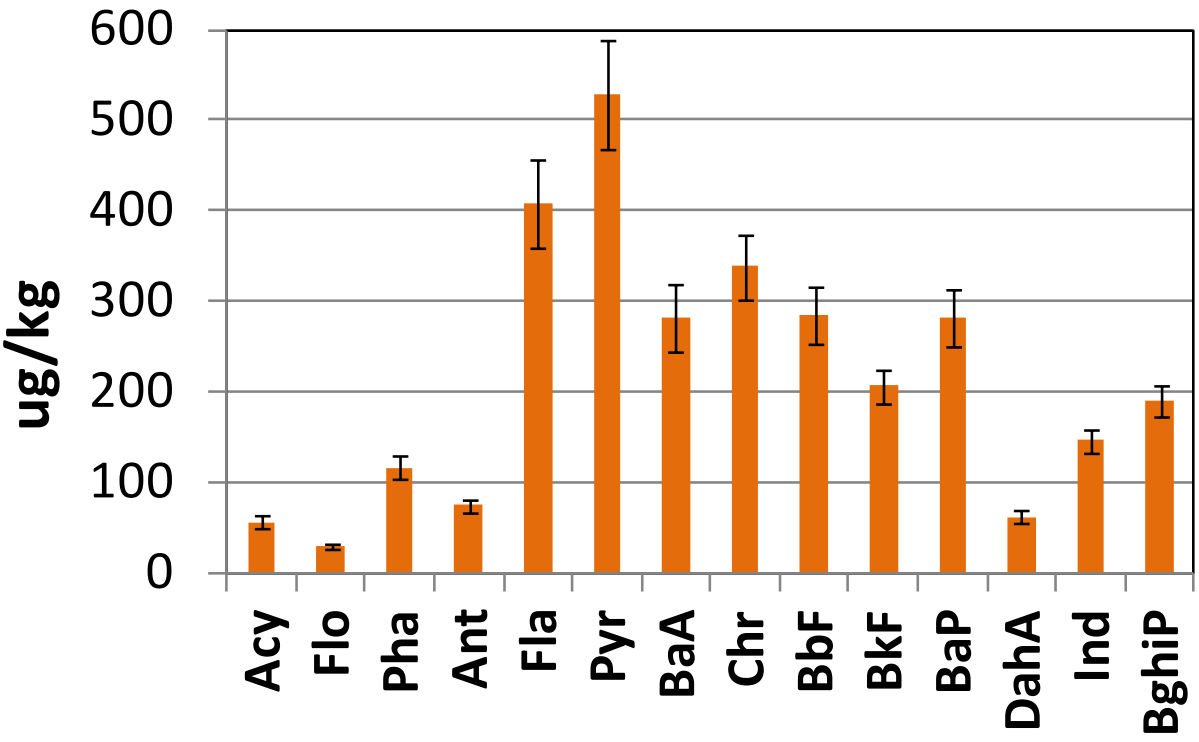

Figure 8. Average PAH profile of IL River sediment cores from all sites (n=80). Error bars represent standard error.

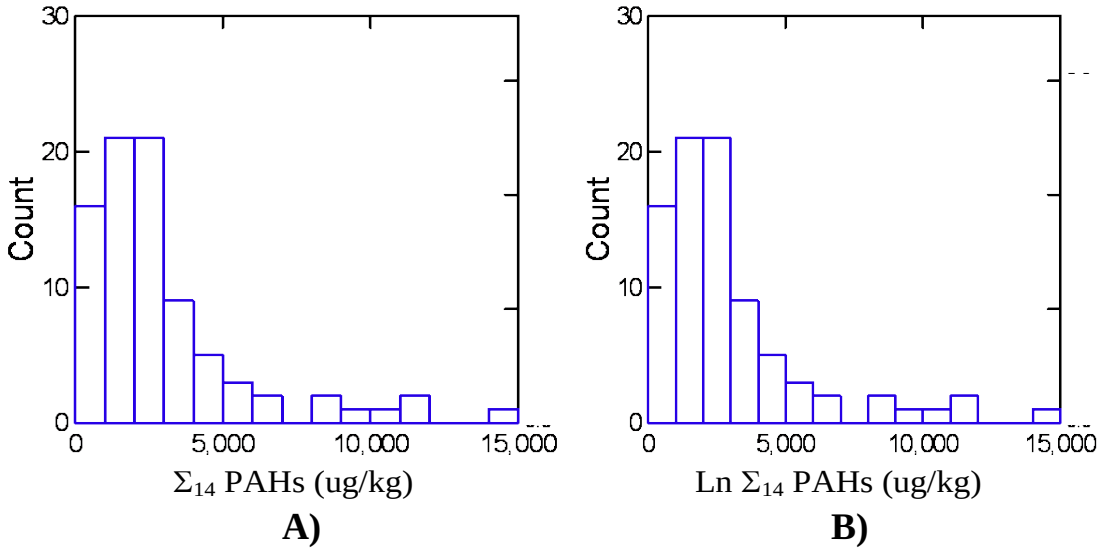

Figure 9. Histograms of Σ_{14} PAH with (A) original and (B) natural log-transformed data, indicating log-normal distribution of PAHs in Illinois River sediment. (n=80)

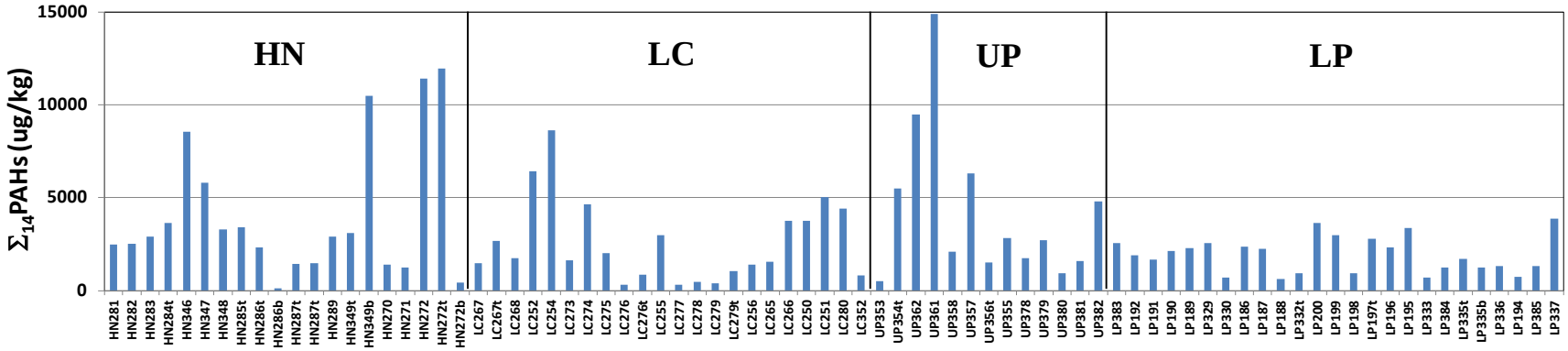

Figure 10. Total (Σ_{14}) PAHs for all samples (n=80) plotted roughly in transect from upstream to downstream.

Total Σ_{14} PAH concentrations were highest at UP (4224 µg/kg) and lowest at LP (1923 µg/kg) (Figure 11). The relative PAH distribution in each reach was very similar, with four-ring PAHs comprising the majority of the total. These results may suggest similar sources and differential transport of PAHs to reaches of the Illinois River.

Of the 80 core samples, only 15 top segments and four bottom segments were reported in this study (see Table 2). Σ_{14} PAHs in top segments were not statistically different from those in whole cores, but were significantly different at the 95% CL from Σ_{14} PAHs in all bottom cores except sample HN349b (Figure 12). At average depths of 144 cm to 226 cm, bottom cores that represent older sediment had significantly less PAH input (with the exception of HN349b). Once again all cores had relatively similar PAH distributions.

Comparison of individual PAHs in upper and lower core segments at each site where pairs are available further indicated that PAH deposition in the past was lower (Figure 13). In three out of the four cases (HN286, HN272, and LP335) PAHs were greatly enriched in upper segments (i.e. all data were well below the 1:1 line). It is unclear why HN349 contains roughly five-fold higher PAH levels in the bottom core segment than the top.

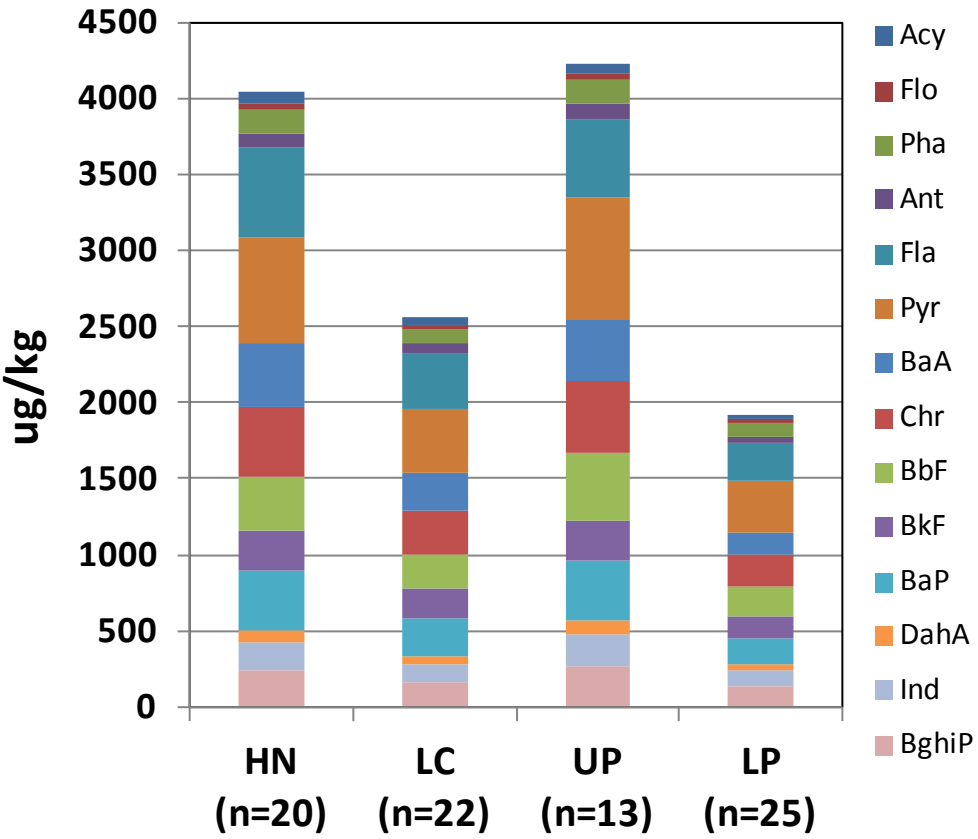

Figure 11. Mean PAH levels and distribution at sampling reaches.

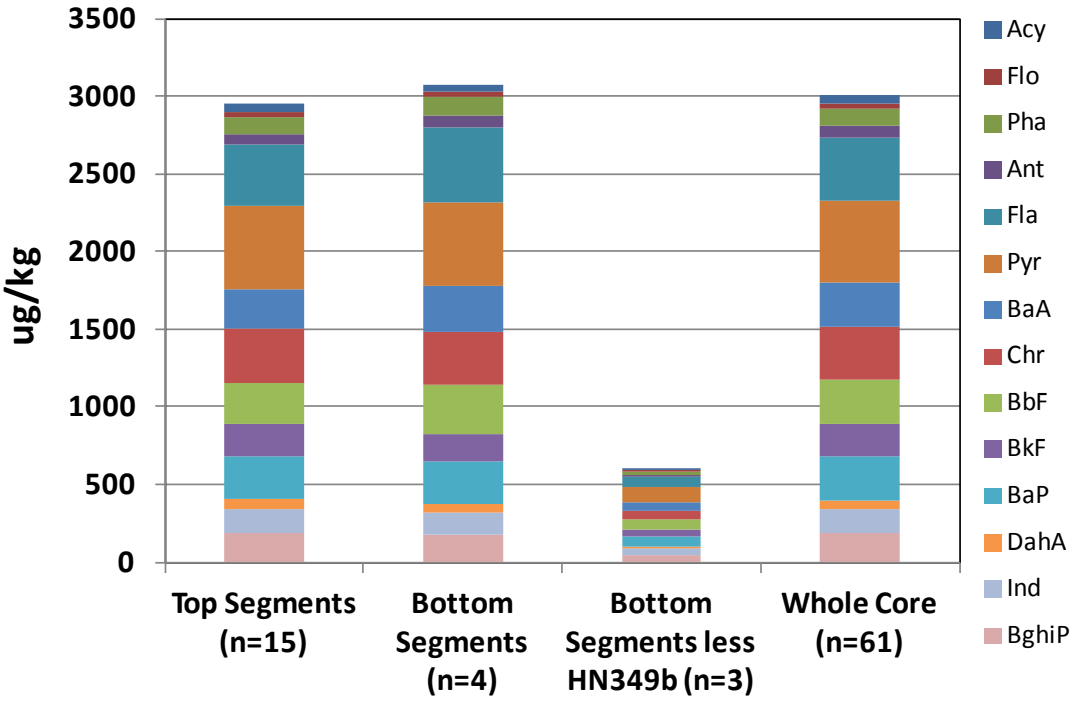

Figure 12. Mean PAH levels and distribution for top segments, bottom segments, and whole cores.

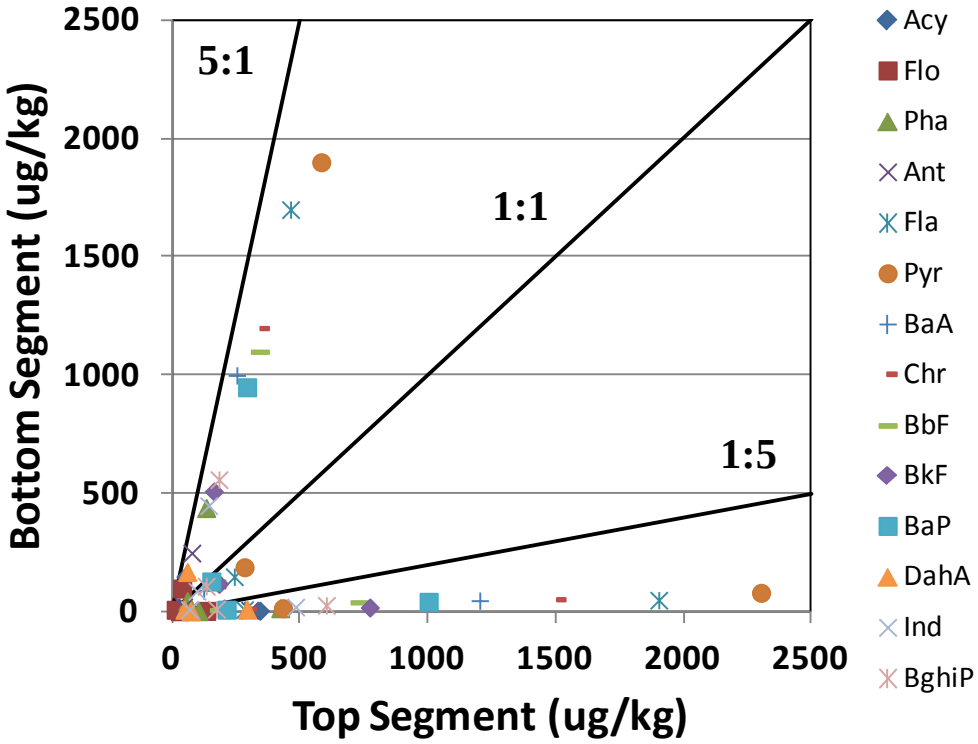

Figure 13. PAH differences between paired top and bottom segments. Points below the 1:1 line indicate higher PAH levels in top segments of cores than bottom. Points above the 1:1 line indicate higher levels in bottom segments.

PMF model performance and sensitivity analysis. Diagnostics for the two-, three-, and four-source PMF solutions are shown for both the 14x80 and the 14x84OUT datasets in Table 7. When unstable, solutions with the lowest Q value are shown. PMF solutions for the 14x80 and the 14x84OUT datasets are quite similar with only minor differences in source contributions and diagnostic values (Table 7), indicating that a small number of outliers and low-detect samples do not strongly influence results. In both cases the improvement in fit (CODs approaching to 1) and decrease in Q is more significant when increasing from two to three sources than when further increasing from three to four sources. The three-source solution has CODs > 0.89, the Exner function < 0.04, and a recalculated relative error of 0.227; indicating an adequate reconstruction of the measured data matrix.

Sensitivity of the PMF model output to different techniques for non-detect reporting were investigated using the 14x84ND dataset and the 15x84 dataset including Ace (Table 8). Unlike the previous sensitivity analysis, the method of non-detect replacement has a strong effect on the PMF model output, despite non-detects only comprising < 6% of the data. This is demonstrated by varied contributions and much higher Q values (Table 8); requiring higher source numbers to achieve reasonable relative errors compared to results in Table 7. The findings demonstrate that the 14x84ND dataset is not well-conditioned for PMF due to greater frequency of repeating values (i.e. all non-detects for a compound have the same value). Furthermore, this method does not make use of RL and MDL information inherent in the approximate data reported for every sample, resulting in a dataset less reflective of the true variation. The PMF output using the 15x84 dataset also yields altered contributions compared to the 14x80 dataset, particularly for the four-source solution (Table 8). Clearly Ace is not fit well based on the low COD value (which does not rise above 0.80 until a seven-source solution is reached) and retaining it in the analysis is not justified given its low discriminative capacity in the source profiles. PMF solution profile correlations of the base 14x80 dataset with the datasets used in sensitivity analysis (14x84OUT, 14x84ND, and 15x84) are shown in Table 9. As expected, 14x84OUT profiles are very similar to 14x80 profiles for all source number solutions, while 14x84ND and 15x84 profiles are much more variable. Thus the PMF model output was not significantly impacted by the inclusion of a few outliers and highly non-detect cores (14x84OUT), but was impacted by the inclusion of an infrequently-detected compound (15x84) and by using a constant non-detect replacement method (14x84ND).

Table 7. PMF model diagnostics and sensitivity analysis with different sample numbers.

Dataset	14x80[a]			14x84OUT[b]		
Source number solution	Two	Three[c]	Four[c]	Two	Three	Four[c]
% Source Contributions	74, 26	48, 27, 25	42, 29, 19, 10	74, 26	47, 28, 25	43, 29, 20, 8
Objective Function Q[d]	1315.09	693.85	552.69	1418.79	765.06	607.61
Relative Error (RE)[e]	.297	0.227	0.215	.301	0.233	.220
Degrees of Freedom (*v*)[f]	932	838	744	980	882	784
Exner Function[g]	.0398	0.0341	0.0256	.0426	0.0314	0.0228
Coefficients of Determination (CODs)[h]						
Acy	.87	.98	.99	.90	.97	.99
Flo	.89	.89	.90	.94	.94	.94
Pha	.87	.89	.91	.94	.93	.94
Ant	.97	.97	.97	.98	.97	.96
Fla	.97	.97	.99	.98	.96	.99
Pyr	.97	.97	.97	.99	.98	.98
BaA	.87	.89	.90	.90	.94	.94
Chr	.97	.96	.97	.93	.95	.95
BbF	.92	.96	.98	.87	.97	.98
BkF	.93	.93	.97	.93	.93	.98
BaP	.97	.97	.97	.98	.98	.98
DahA	.93	.95	.96	.93	.96	.97
Ind	.97	.98	.99	.97	.99	.99
BghiP	.95	.96	.97	.96	.98	.98

[a] Dataset 14x80 from Table 2.
[b] Dataset 14 x 18OUT with outlier and low-detect samples retained.
[c] Solution instability. Chosen solution has the lowest Q value, or if Q values have < 1% difference is the most frequently generated solution.
[d] Based on 0.25 RE of measurements.
[e] Recalculated by setting Q = *v*.
[f] *v* calculated by m*n+p(n+m).
[g] Best fit at 0.
[h] Best fits at 1.

Table 8. PMF model diagnostics for sensitivity analysis with a different non-detect substitution method and analyte number.

Dataset	14x84ND[a]				15x84[b]		
Source number	Two[c]	Three[c]	Four		Two	Three	Four[c]
% Source	69, 31	39, 36, 25	37, 35, 19, 9		74, 26	42, 33, 25	57, 20, 19, 4
Objective Function	3511.56	2695.13	1484.07		1667.33	1016.70	632.68
Relative Error (RE)[e]	.473	0.437	.344		.313	0.257	.214
Degrees of Freedom	980	882	784		1062	963	864
Exner Function[g]	.0842	0.0359	0.0335		.0428	0.0345	0.0331
Coefficients of Determination (CODs)[h]							
Acy	.89	.97	.98	Acy	.90	.98	.98
Flo	.90	.90	.98	Flo	.95	.96	.98
Pha	.90	.93	.96	Pha	.94	.95	.94
Ant	.97	.98	.97	Ant	.98	.97	.96
Fla	.88	.97	.97	Fla	.95	.95	.97
Pyr	.95	.98	.98	Pyr	.99	.99	.98
BaA	.82	.91	.92	BaA	.90	.93	.92
Chr	.90	.93	.94	Chr	.93	.95	.94
BbF	.94	.96	.96	BbF	.86	.90	.95
BkF	.68	.93	.93	BkF	.93	.93	.94
BaP	.97	.97	.98	BaP	.98	.98	.98
DahA	.89	.95	.96	DahA	.93	.95	.96
Ind	.89	.99	.99	Ind	.97	.98	.99
BghiP	.87	.98	.98	BghiP	.96	.97	.98
				Ace	.72	.74	.80

[a] Dataset 14x84ND has non-detects substituted with half the lowest value for each analyte.
[b] Dataset 15x84 includes Ace (infrequently detected) PAH.
[c] Solution instability. Chosen solution has the lowest Q value, or if Q values have < 1% difference is the most frequently generated solution.
[d] Based on 0.25 RE of measurements.
[e] Recalculated setting Q = *v*.
[f] *v* calculated by m*n+p(n+m).
[g] Best fit at 0.
[h] Best fits at 1.

Table 9. Pearson correlation coefficients between PMF solution profiles of the base (14x80) and varied datasets.[a]

		14x80										
		Two			Three				Four			
		74%	*26%*		*48%*	*27%*	*25%*		*42%*	*29%*	*19%*	*10%*
14x84OUT	*74%*	**1.00**	0.21	*47%*	**1.00**	0.73	0.31	*44%*	**1.00**	0.41	0.8	-0.11
	26%	0.23	**1.00**	*28%*	0.73	**0.98**	0.06	*28%*	0.35	**1.00**	0.12	0.09
				25%	0.27	0.13	**1.00**	*19%*	0.78	0.17	**0.98**	-0.25
								9%	-0.16	-0.07	-0.12	**0.99**
14x84ND	*69%*	**0.98**	0.35	*39%*	0.89	**0.91**	0.00	*37%*	**0.90**	0.71	0.63	0.02
	31%	0.39	0.85	*36%*	**0.95**	0.69	0.58	*35%*	**0.92**	0.35	**0.91**	-0.33
				25%	0.22	0.16	**0.99**	*19%*	0.13	0.61	0.09	0.78
								9%	0.16	0.08	0.06	0.55
15x84	*74%*	**1.00**	0.21	*42%*	0.88	**0.96**	0.16	*57%*	**0.95**	0.63	0.72	-0.05
	26%	0.23	**1.00**	*33%*	**1.00**	0.72	0.30	*20%*	0.79	0.21	**0.98**	-0.28
				25%	0.26	0.13	**1.00**	*19%*	0.13	0.55	0.11	0.83
								4%	-0.03	0.43	-0.51	0.03

[a]. Correlation Coefficients > 0.90 bolded. See Tables 7 and.8 for dataset descriptions and two- to four-source solution diagnostics.

PMF source profiles and contributions. The three-source PMF solution from the original 14x80 dataset was chosen for further investigation, as it provided adequate reconstruction of the receptor matrix with the least number of sources and a relatively low recalculated relative error representing analytical, sampling, and environmental uncertainty (0.23) (see Table 7). The primary PAH source (S1) is predicted to contribute 48% of the total PAH mass to the Illinois River and is dominated by Pyr, Fla, and BbF (Figure 14). The second source (S2) is predicted to contribute 27% of the total PAH mass, and is high in Fla and Pyr, as well as other four-ring PAHs. The main differences between S1 and S2 are the presence of Pha in S1, the presence of Acy and DahA in S2, and higher proportions of Pyr to Fla and BbF to BkF in S1 compared to S2. The third source (S3) is predicted to contribute 25% of the PAH burden (Figure 14). S3 does not contain Fla, but is more uniformly loaded with four- and five-ring PAHs. S3 also has the highest relative BkF through BghiP loadings of all the sources.

PAH contributions from all sources are similar for most samples, but greater peaks and variability are evident for S1 and S2 in certain cores, particularly upstream of LP (Figure 15). Large relative PAH S1 contributions at sites with much higher levels of Σ_{14}PAHs may indicate local and/or point sourcing. Source S3 is least correlated with S1 and S2 at sites LC252, 254 and 256-280 (where it is lower); and sites UP382 and LP329 (where it is higher).

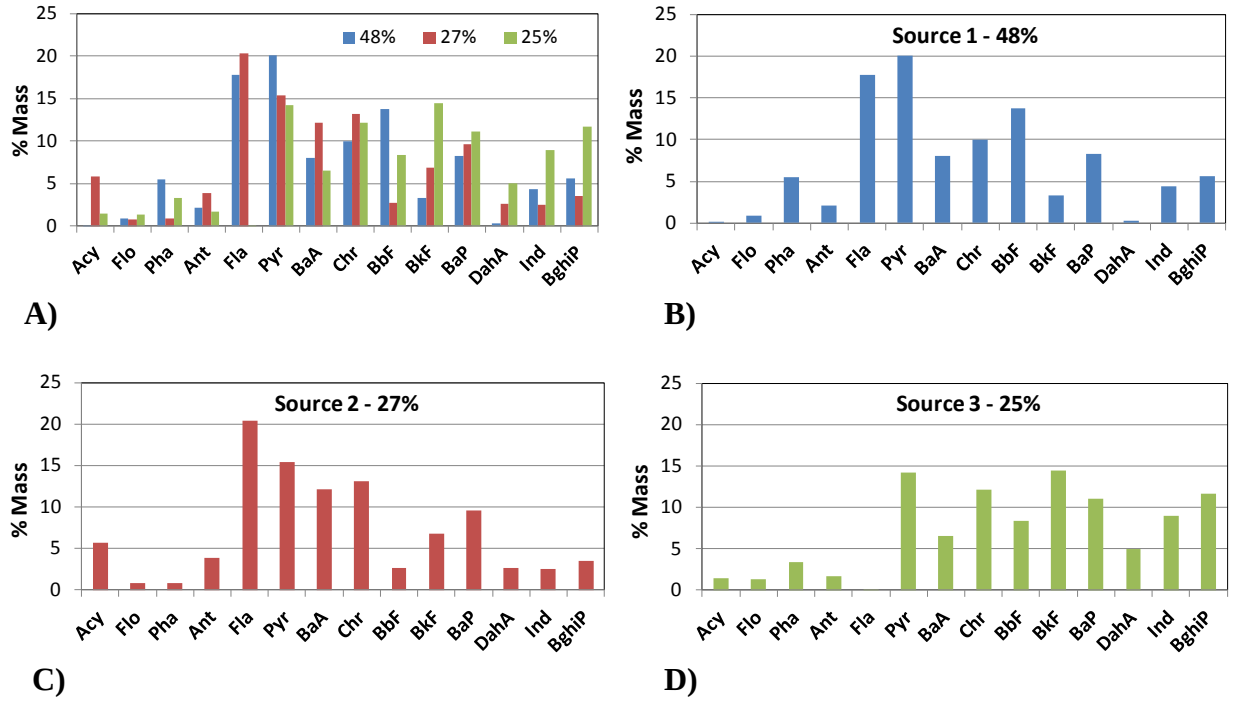

Figure 14. PAH source composition profiles from three-source PMF solution. Profiles shown (A) together and individually for (B) S1, (C) S2, and (D) S3.

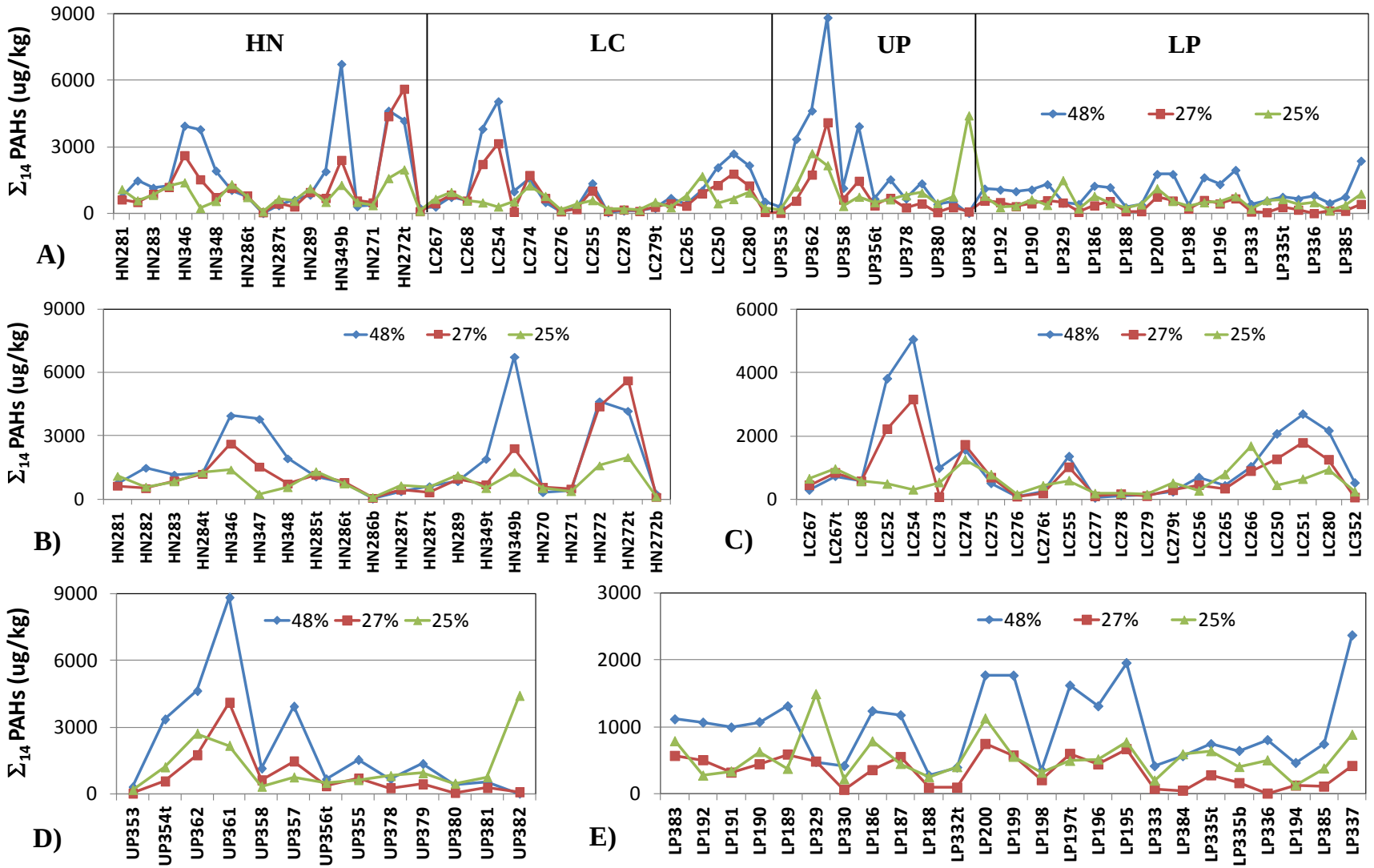

Figure 15. PAH source contributions from three-source PMF solution. The (A) overall source contribution plot is shown in greater detail by (B) HN, (C) LC, (D) UP, and (E) LP reaches. Note different y-axis scales.

Reference profile analysis. Cos φ values between modeled sources (S1-S3) and PAH reference profiles are given in Table 10 (values over 0.95 are in bold). Sources S1 and S2 match lignite and sub-bituminous coal profiles, but not bituminous or anthracite coal profiles. Modeled sources are similar to combustion-derived sources, with particularly strong matches between source S1 and gas engine and between sources S1 and S2 and wood burning (cos φ > 0.92). Gas soot is one of the few compiled reference sources that is more similar to S3 than to S1 or S2. Most modeled sources have PAH profiles that resemble those of Illinois soils, biosolids, urban dust, roadside air, and coal tar related dust from parking lots and driveways (Table 10) but not new oil, used oil, coal tar, or creosote. Source S1 is very similar to background soil, coal tar sealcoat dusts, and biosolids (cos φ > 0.95), S2 is most like coal tar sealcoat dust (cos φ > 0.95), and S3 is most strongly related to roadside air (cos φ > 0.90). Thus PMF results suggested that a mixed upland source and coal or wood-derived sources such as coal tar sealcoat (sources S1 and S2, 75%) are major contributors to sediment PAHs in the Illinois River, as well as a traffic-based roadside air source (S3, 25%). Another conclusion from these observations is that the majority of reference sources are similar to modeled sources, making definitive source assignments based solely on cos φ values impossible considering reference profile uncertainties. This is illustrated by the fact that more than half of S1 and S2 comparisons with compiled reference profiles have cos φ values > 0.7 (Table 10). For this reason coal dust was not uniquely resolved from the coal-derived sources and thus could not be assessed for reduced PAH bioavailability. In addition, the overall lack of naphthalene in these sediments (which is a major component of coal), is not consistent with the presence of coal in sediments.[35]

To be able to interpret the PMF results, we must first understand the nature of PAH sources to the sediment. Possible sources of PAHs to the sediment include direct discharges (wastewater, transport spills), as well as sedimentation from the upper watershed and tributaries, and erosion of agricultural soils. The soil may have acquired PAHs via atmospheric deposition, open/biomass burning, equipment use, or biosolids application. While exposed to air and sunlight, soils undergo particle aging that may alter the original source profile. Furthermore, PAH accumulation in sediments is determined by sediment composition, black carbon content, and organic content or grain size.[11] The agricultural nature of the Illinois River watershed, mixture of different sediment types, and various transport pathways (including PAH incorporation into soil subsequently eroded and deposited in sediments) may inhibit clear resolution of sources.

Comparison of PAH source apportionment in other sediment studies. A number of studies have analyzed sources of PAHs to different lacustrine, marine, and riverine sediment environments using various source apportionment and receptor modeling techniques. The majority of PAHs in sediments in Lake Calumet in Chicago, IL, USA have been sourced to traffic and coke oven emissions utilizing both Chemical Mass Balance[20] and factor analysis based receptor models.[17] A recent source apportionment analysis of PAHs in suburban lake sediment throughout the USA concluded that the majority of PAHs are now derived from use of the coal tar sealant, with vehicle sources as the second most important source.[51] This study did not identify coke ovens as a significant source. PAHs in Lake Michigan sediment were found to be impacted by traffic, coal (coke), and wood burning sources in an analysis of dated sediment cores.[52] Marine sediments near Victoria, BC, Canada were reported to contain PAHs related to wood combustion, coal, coke, petroleum combustion, and traffic related sources from atmospheric deposition, stormwater runoff, and wastewater discharges.[15] The Fraser River basin was found to be impacted by a variety of

sources dominated by petroleum combustion sources near urban areas, and biomass combustion in remote areas.[10] A source apportionment study of PAHs in sediment cores of the Kinnickinnic River, WI concluded coke oven, coal tar/coal wood gasification, and highway dust were the most important contributors of PAHs over time.[22] Primary PAH sources to Black River sediments and Ashtabula River sediments in Ohio were found to be traffic, next coke oven, and finally wood burning/coal tar related.[18]

Most of the above-referenced studies utilized significant amounts of external information to make these conclusions, such as sediment characteristics, sediment dating, source sampling, and detailed watershed knowledge. Resolution of sources in riverine systems can be particularly difficult or even impossible due to differential deposition, mixing, scouring, and resuspension of sediment. In the present study, unique identification of sources in the Illinois River appears to be limited by collinearity of reference sources, lack of local and historical information, lack of core temporal resolution (i.e. modeling of core composites), and complexities in the source-receptor pathway.

Table 10. Cosine φ similarity of PMF modeled and reference PAH source profiles.[a]

Coal

	LigA1	LigA2	SubC1	SubC2	SubB1	SubB2	SubA	HVC	HVB	HVA1	HVA2	MV	LV	Semi	Anth	Coal or coke	Coal dust
S1	0.92	**0.95**	0.87	**0.96**	0.81	0.87	**0.95**	0.67	0.42	0.61	0.35	0.31	0.34	0.54	0.36	0.74	0.58
S2	0.83	0.82	0.80	0.87	0.73	0.82	0.81	0.59	0.30	0.58	0.24	0.19	0.22	0.34	0.21	0.64	0.53
S3	0.52	0.72	0.54	0.69	0.46	0.47	0.74	0.41	0.34	0.43	0.28	0.24	0.31	0.51	0.27	0.61	0.45

Combustion

	Coke Oven	Power Plant	Residential	Ave Coal	Gas Engine	Diesel Engine	Ave Gas & Diesel	Traffic Tunnel	Ave Petroleum	Wood Burning	Gas Soot	Diesel Soot	Diesel Particulate	Diesel Equip.
S1	0.86	0.89	0.66	0.90	**0.94**	0.81	0.88	0.90	0.91	**0.94**	0.63	0.75	0.72	0.58
S2	0.82	0.86	0.58	0.82	0.86	0.74	0.80	0.81	0.82	**0.92**	0.54	0.65	0.62	0.44
S3	0.87	0.66	0.38	0.70	0.80	0.47	0.57	0.88	0.70	0.62	0.79	0.58	0.41	0.46

Oil, coal tar (CT), traffic, and other

	Bio-solids	New Oil	Used Oil	Coal Tar (CT)	Creosote (CT)	CT Seal Dust A	CT Seal Dust B	CT Seal Parking Lot Dust	CT Seal Drv-way Dust	Street Dust by CT Lots	Street Dust	Tire Debris	Used Crank case Oil	Asphalt	Road-side Air	Urban Dust	Back-ground Soil[b]
S1	**0.96**	0.45	0.61	0.69	0.39	**0.95**	**0.98**	**0.96**	0.93	**0.96**	0.94	0.81	0.72	0.82	0.75	0.94	**0.95+/-.01**
S2	0.91	0.27	0.51	0.67	0.34	0.90	**0.96**	0.87	0.86	0.87	0.91	0.73	0.64	0.70	0.63	0.80	0.90+/-.01
S3	0.80	0.33	0.49	0.45	0.31	0.61	0.73	0.61	0.55	0.64	0.65	0.62	0.50	0.76	**0.93**	0.76	0.77+/-.02

[a] Cos φ values above 0.95 or best fits > 0.90 for each source are bold. See Tables 4 through 6 for reference profile information and Figure 14 for modeled profiles S1 (48%), S2 (27%), and S3 (25%).

[b] Soil background profile average +/- standard deviation from Chicago, other metropolitan, and non-metropolitan areas (Table 1).

Ratio analysis. PAH ratios were calculated from sediment measurements and compared to diagnostic ratio domains to estimate the predominant PAH sources to Illinois River sediment. Site-averaged Illinois River sediment PAH data generally cluster in ratio domains consistent with combustion (Figure 16). The main exception is the Fla/Fla+Pyr ratio which places UP in the petroleum source domain. River reaches are likely to represent areas with similar hydrologic and watershed characteristics and thus have similar non-local PAH sources, and diagnostic ratio results indicating combustion-derived sources support this expectation. Ratios distinguishing between petroleum and coal/biomass combustion (Fla/Fla+Pyr and Ind/Ind+BghiP) indicate petroleum combustion, although 'updated' Ind/Ind+BghiP ranges signify coal or biomass combustion.

The observed variability among ratios (particularly for Fla/Fla+Pyr and Ind/Ind+BghiP) for reported samples casts some doubt on the ability of the ratio method to accurately and uniquely identify sources (Figure 16). In fact for all ratios, a number of petroleum samples appear in the petroleum combustion domain and even in the coal/biomass combustion domains. Conversely, combustion samples can also be found in conflicting petroleum domains. However, contradictory results utilizing different diagnostic ratios does not necessarily mean the results are incorrect; they may reflect a distribution of overlapping contributions of PAHs from particular sources to the total PAH mass, as shown by the PMF results discussed above. Illinois River PAH ratios are similar to those for a number of petrogenic and combustion sample types, except for the Ant/Ant+Pha ratio that computes higher values in sediments (toward the combustion range) than in reference samples (Figure 16).

PAH ratios in sediments from all cores as well as modeled profiles from the PMF three-source solution (S1, S2, and S3) are shown together in Figure 17. PAH ratios in cores are generally similar within, as well as between sites. S1 clusters with samples in the petroleum combustion region, while S2 and S3 deviate from the sample cluster for lower molecular weight ratios Ant/Ant+Pha and Fla/Fla+Pyr, respectively. The Ind/Ind+BghiP, BaA/BaA+Chr, and Ant/Ant+Pha ratios indicate all modeled sources are combustion-derived. In contrast, the Fla/Fla+Pyr ratio places sources S1, S2, and S3 in petroleum combustion, coal/biomass combustion, and petroleum domains, respectively (Figure 17). The ratios Ant/Ant+Pha and BaA/BaA+Chr suggest contributions from bituminous coal sources to the Illinois River sediments, however PMF modeled sources do not fall within any coal ratio ranges. Ratio analysis suggests modeled sources are combustion-derived with possible petroleum influence on S3. However, variability between and ambiguity within ratios prevents clear or detailed source assignment.

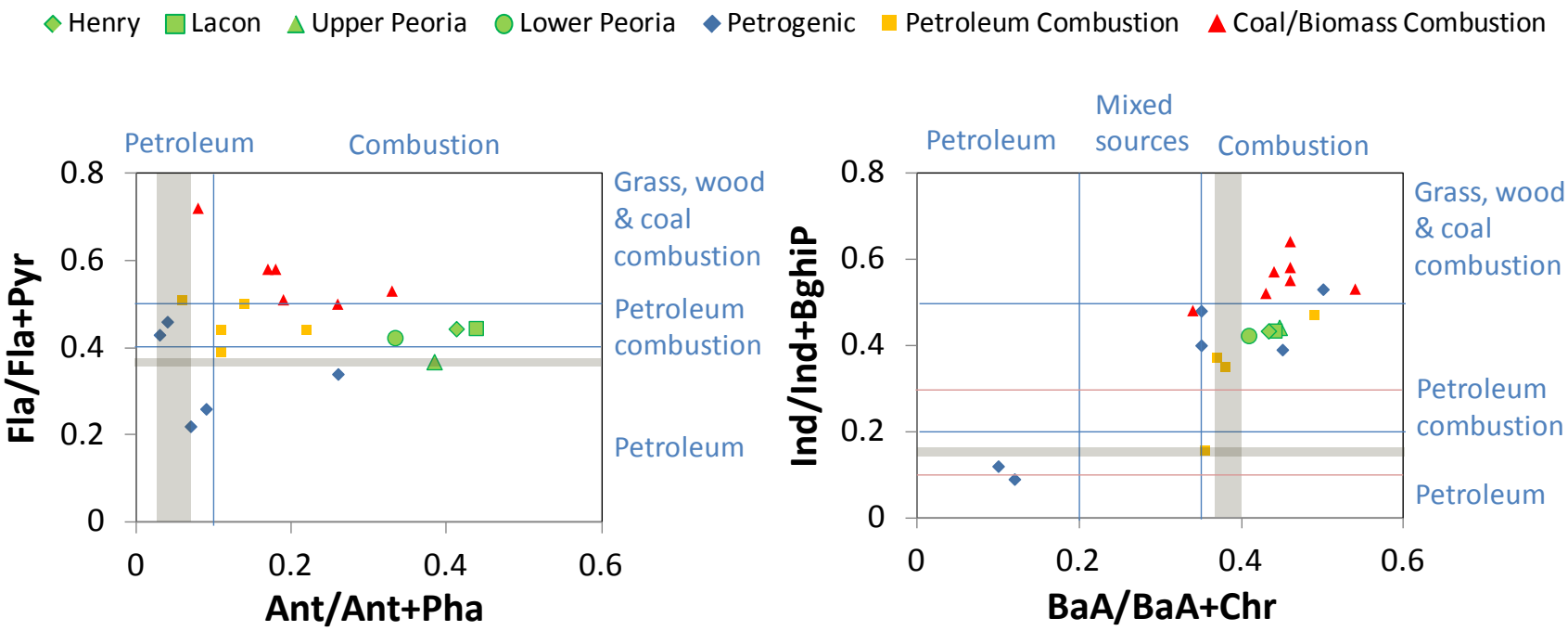

Figure 16. PAH diagnostic ratio plots of site-averaged Illinois River sediment and literature-compiled petrogenic and combustion samples from Table 3. Source ranges are delineated in blue from Yunker et al. (2002)[10] according to Table 3. Shaded gray indicates coal domains of bituminous coal samples and pink lines delineate recently updated source ranges for Ind/Ind+BghiP from Yunker et al. (2012).[15]

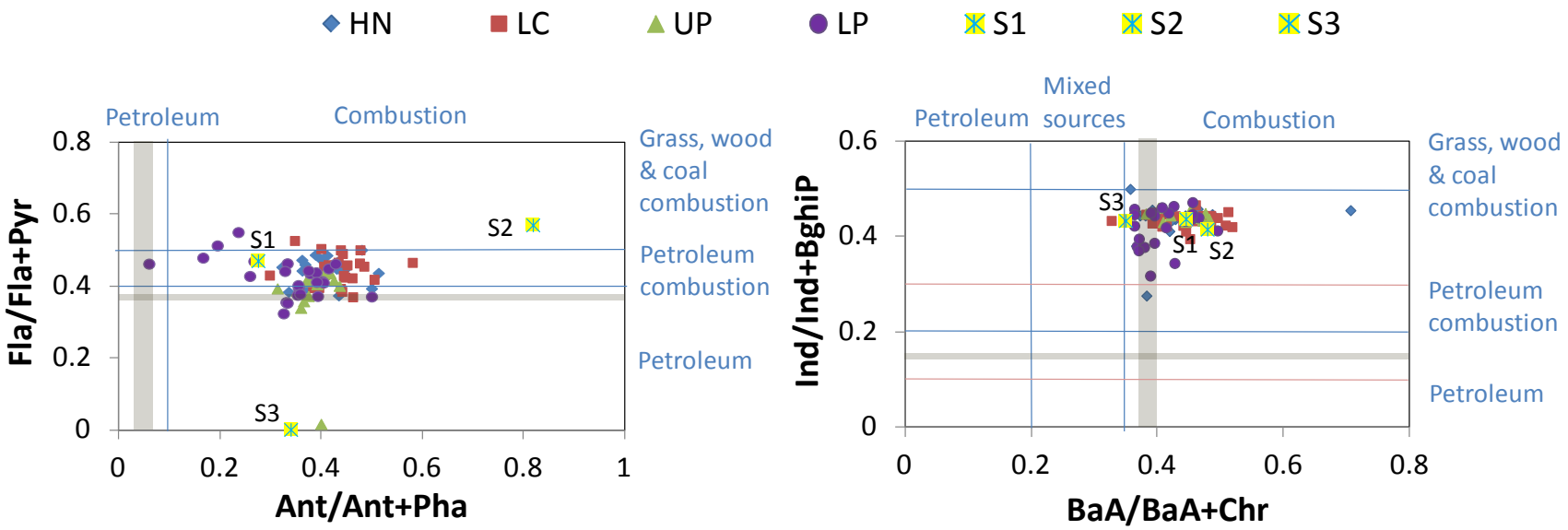

Figure 17. PAH diagnostic ratio plots of Illinois River sediment samples and PMF modeled sources. Source ranges are delineated in blue from Yunker et al. (2002)[10] according to Table 3. Shaded gray indicates coal domains of bituminous coal samples and pink lines delineate recently updated source ranges for Ind/Ind+BghiP from Yunker et al. (2012).[15]

PAH ratios of reference sources obtained from the literature (Figure 18) are not always consistent with the source identified by the diagnostic ratio domains. For instance Fla/Fla+Pyr indicates a petroleum non-combustion source for gas engine emissions and a coal/biomass combustion source for diesel engine emissions. All ratios indicate a combustion source for used lubricating oil. Many samples such as processed or weathered materials do not fit uniformly in a given ratio space. For example, the PAH ratios in parking lot dust, tire debris, and biosolids appear in conflicting diagnostic domains and clearly lack specificity. This represents a limitation of the ratio method for detailed source apportionment analysis. PAH ratios in coals generally distribute across the ratio domains, with semi-anthracite appearing in petroleum regions and lignite appearing in the combustion regions (Figure 18). Bituminous coal overlaps with the semi-anthracite, sub-bituminous, and lignite for Ant/Ant+Pha, Fla/Fla+Pyr, and BaA/BaA+Chr ratios, respectively. Based on varying PAH distributions with coal rank, the ratio plots as well as other diagnostic parameters[35] cannot uniquely represent fossil coal for determination of coal particles in sediment. Modeled sources have higher Ant/Ant+Pha diagnostic ratios than most reference sources, appearing well within the combustion range (note S2 is not visible in Figure 18 as described in caption, but can be seen in Figure 17). Overestimation of Pha loading in environmental samples by mass balance receptor models using similar source profiles has been observed previously.[19, 21] The observed lack of measured Pha in the present study, and thus lower Ant/Ant+Pha ratios, might be due to the increased mobility and/or degradation of Pha relative to Ant in the sediment. In fact, faster desorption and microbial degradation of Pha relative to Ant in soil has been reported to change the original profile or ratio.[11] The lability of low molecular weight PAHs in soil or sediments may render this ratio less reliable as a diagnostic tool.

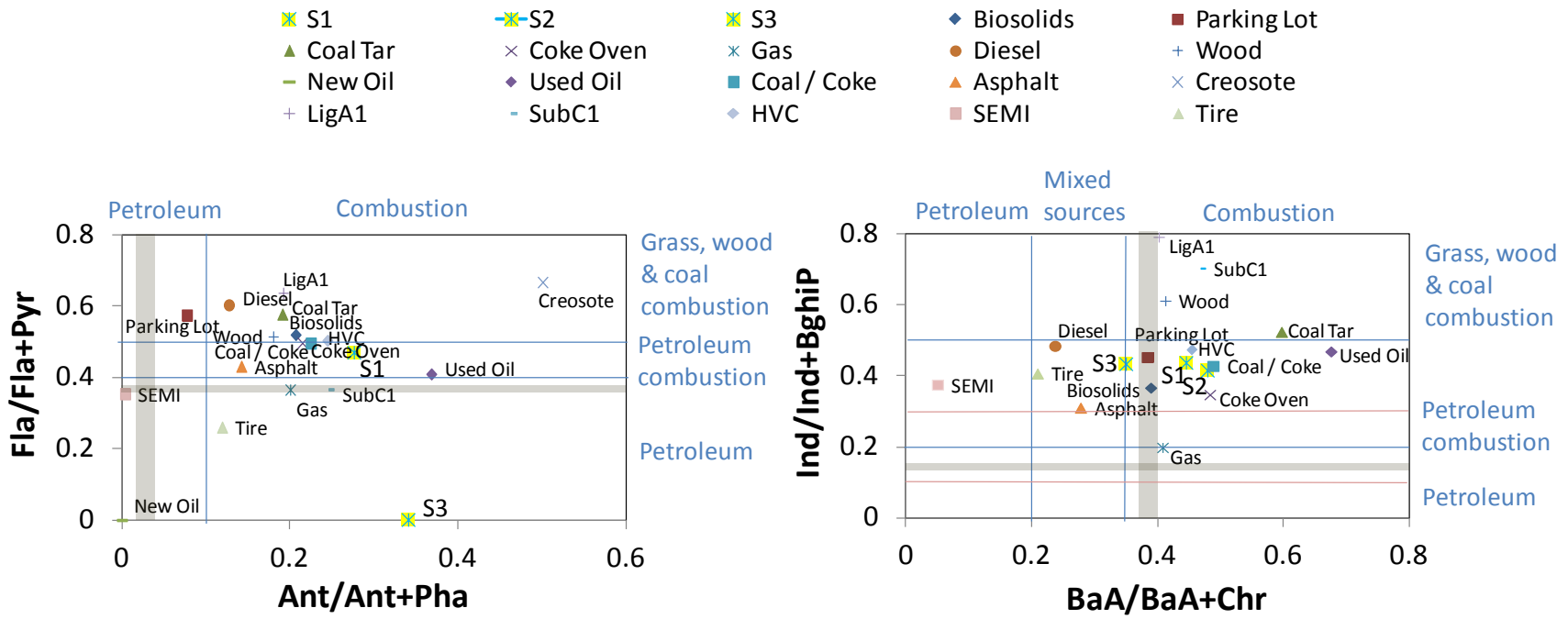

Figure 18. PAH diagnostic ratio plots of select reference sources and PMF modeled sources. Source ranges are delineated in blue from Yunker et al. (2002)[10] according to Table 3. Shaded gray indicates coal domains of bituminous coal samples and pink lines delineate recently updated source ranges for Ind/Ind+BghiP from Yunker et al. (2012).[15] S2 has an Ant/Ant+Pha ratio of 0.82 (combustion) and a Fla/Fla+Pyr ratio of 0.57 (coal/biomass combustion) and is not shown on the left plot in order to better observe reference sources (see instead Figure 17).

CONCLUSIONS AND IMPLICATIONS

PMF results suggested that a mixed upland source and coal-derived sources like coal tar sealcoat (sources S1 and S2, 75%) are major contributors to sediment PAHs in the Illinois River, as well as a diffuse traffic-based source (S3, 25%). The best fit predictions for PMF profiles identified lignite or sub-bituminous coal sources, biosolids, coal-tar sealcoat dust, and/or background soil sources for S1, the predominant PAH source to the Illinois River sediments. Coal dust was not uniquely resolved from the coal-derived sources, however, and thus could not be assessed for reduced PAH bioavailability. The second most important source was most closely associated with coal tar sealcoat dust. The third source did not match with any source with $\cos \varphi > 0.95$, but matched traffic-related roadside air with $\cos \varphi > 0.90$. None of the source profiles indicated significant petroleum inputs to sediments.

Due to reference source similarity and complex PAH source-receptor pathways, these predicted sources of PAHs to the Illinois River must be confirmed using additional site-specific source information. The proximity of core locations to anthropogenic sources and activities may be examined (e.g. distances from towns, shorelines, main channel, harbors, docks, and coal stockpiles) and compared to PMF contribution results to aid source identification. A more definitive source apportionment analysis is also possible by increasing the number of PAHs in the dataset beyond the typical PAH priority pollutant list to better represent coal and other sources not clearly defined by priority PAHs alone, and gaining further resolution with additional core dating, depth, sediment characterization, and analytical uncertainty information.

The existing dataset was prepared for PMF by removing samples and analytes over 40% non-detect and identified outliers and replacing non-detects with half the lowest analyte value (approximating the MDL) for each sample. The sensitivity analysis demonstrated that PMF was robust to minor additions of oulier and low-detect samples, mildly robust to the addition of an infrequently detected analyte, and least robust to other methods of non-detect replacement. This has important implications for use of PMF in subsequent source apportionment studies. The results indicate that non-detect estimation decreases certainty of the output in spite of the increasing degrees of freedom obtained by adding more data. Estimating non-detects with many constant values is particularly problematic for PMF and less desirable than a method that retains variation in the data.

The use of PAH diagnostic ratios predicted petroleum combustion input to Illinois River sediment, but significant limitations of the method decrease confidence in the results. Inconsistent results from the four diagnostic ratios with the sediment data and contradictory identification of literature-compiled environmental samples and reference profiles indicate all ratios are not accurate or reliable for all sources. Diagnostic ratio accuracy was notably poor for sources with different degrees of aging (used versus new oil, coal tar parking lot dust versus coal tar) and for fossil coal sources whose ratios were distributed across all domains and were not uniquely represented. Ratios can also be misleading if samples are impacted from more than one source, indicating only a dominant source or a mixture of sources inaccurately. For example, PAH ratios may indicate petroleum combustion inputs to Illinois River sediment even though they represent a combination of coal tar sealcoat, traffic, and other uncombusted or coal/biomass combustion sources as shown

by PMF analysis. The results of this study demonstrate that PMF analysis is a more accurate method than diagnostic ratio analysis for performing a detailed, quantitative, multiple-source apportionment study.

CITED LITERATURE

(1) Demissie, M.; Xia, R.; Keefer, L.; Bhowmik, N. *The Sediment Budget of the Illinois River*. Illinois State Water Survey, Contract Report 2004-13, Champaign, IL: **2004**.

(2) Machesky, M. L.; Slowikowski, J. A.; Cahill, R. A.; Bogner, W. C.; Marlin, J. C.; Holm, T. R.; Darmody, R. G. Sediment Quality and Quantity Issues Related to the Restoration of Backwater Lakes Along the Illinois River Waterway. *Aquatic Ecosystem Health & Management*: **2005**, *8* (1), 33-40.

(3) Baek, S. O.; Field, R. A.; Goldstone, M. E.; Kirk, P. W.; Lester, J. N.; Perry, R. A Review of Atmospheric Polycyclic Aromatic-Hydrocarbons - Sources, Fate and Behavior. *Water Air and Soil Pollution*: **1991**, *60* (3-4), 279-300.

(4) Cahill, R. A.; Salmon, G. L.; Slowikowski, J. A.; Salmon, G. L. *Lakes along the Illinois River*. Illinois Sustainable Technology Center, Champaign, IL: **2008**.

(5) Slowikowski, J. A.; Larson, B. D.; Russell, A. M. *Database Development to Support Sediment Characterization of the Middle Illinois River*. Illinois State Water Survey, Champaign, IL: **2008**.

(6) Tiered Approach to Corrective Action Objectives. In *35 IL Adm. Code Part 742*, **2007**.

(7) Shor, L. M.; Kosson, D. S.; Rockne, K. J.; Young, L. Y.; Taghon, G. L. Combined Effects of Contaminant Desorption and Toxicity on Risk from PAH Contaminated Sediments. *Risk Analysis*: **2004**, *24* (5), 1109-1120.

(8) Rockne, K. J.; Shor, L. M.; Young, L. Y.; Taghon, G. L.; Kosson, D. S. Distributed Sequestration and Release of Pahs in Weathered Sediment: The Role of Sediment Structure and Organic Carbon Properties. *Environmental Science & Technology*: **2002**, *36* (12), 2636-2644.

(9) Demissie, M.; Bhowmik, N. *Peoria Lake Sediment Investigation*. Illinois State Water Survey, Surface Water Section at the University of Illinois, Champaign, IL: **1986**.

(10) Yunker, M. B.; Macdonald, R. W.; Vingarzan, R.; Mitchell, R. H.; Goyette, D.; Sylvestre, S. PAHs in the Fraser River Basin: A Critical Appraisal of PAH Ratios as Indicators of PAH Source and Composition. *Organic Geochemistry*: **2002**, *33* (4), 489-515.

(11) Tobiszewski, M.; Namieśnik, J. PAH Diagnostic Ratios for the Identification of Pollution Emission Sources. *Environmental Pollution*: **2012**, *162* 110-119.

(12) Ravindra, K.; Sokhi, R.; Van Grieken, R. Atmospheric Polycyclic Aromatic Hydrocarbons: Source Attribution, Emission Factors and Regulation. *Atmospheric Environment*: **2008**, *42* (13), 2895-2921.

(13) Kim, D.; Kumfer, B. M.; Anastasio, C.; Kennedy, I. M.; Young, T. M. Environmental aging of polycyclic aromatic hydrocarbons on soot and its effect on source identification. *Chemosphere*: **2009**, *76* (8), 1075-1081.

(14) Steinhauer, M. S.; Boehm, P. D. The Composition and Distribution of Saturated and Aromatic-Hydrocarbons in Nearshore Sediments, River Sediments, and Coastal Peat of the Alaskan Beaufort Sea - Implications for Detecting Anthropogenic Hydrocarbon Inputs. *Marine Environmental Research*: **1992**, *33* (4), 223-253.

(15) Yunker, M. B.; Perreault, A.; Lowe, C. J. Source Apportionment of Elevated PAH Concentrations in Sediments Near Deep Marine Outfalls in Esquimalt and Victoria, BC, Canada: Is Coal from an 1891 Shipwreck the Source? *Organic Geochemistry*: **2012**, *46* 12-37.

(16) Sofowote, U. M.; McCarry, B. E.; Marvin, C. H. Source Apportionment of PAH in Hamilton Harbour Suspended Sediments: Comparison of Two Factor Analysis Methods. *Environmental Science & Technology*: **2008**, *42* (16), 6007-6014.

(17) Bzdusek, P. A.; Christensen, E. R.; Li, A.; Zou, Q. M. Source Apportionment of Sediment PAHs in Lake Calumet, Chicago: Application of Factor Analysis with Nonnegative Constraints RID A-3395-2008. *Environmental Science & Technology*: **2004**, *38* (1), 97-103.

(18) Christensen, E. R.; Bzdusek, P. A. PAHs in Sediments of the Black River and the Ashtabula River, Ohio: Source Apportionment by Factor Analysis. *Water Research*: **2005**, *39* (4), 511-524.

(19) Li, K.; Christensen, E. R.; Van Camp, R. P.; Imamoglu, I. PAHs in Dated Sediments of Ashtabula River, Ohio, USA. *Environmental Science & Technology*: **2001**, *35* (14), 2896-2902.

(20) Li, A.; Jang, J. K.; Scheff, P. A. Application of EPA CMB8.2 Model for Source Apportionment of Sediment PAHs in Lake Calumet, Chicago RID A-3395-2008. *Environmental Science & Technology*: **2003**, *37* (13), 2958-2965.

(21) Van Metre, P. C.; Mahler, B. J. Contribution of PAHs from Coal–Tar Pavement Sealcoat and other Sources to 40 US Lakes. *Science of the Total Environment*: **2010**, *409* (2), 334-344.

(22) Christensen, E. R.; Li, A.; AbRazak, I. A.; Rachdawong, P.; Karls, J. F. Sources of Polycyclic Aromatic Hydrocarbons in Sediments of the Kinnickinnic River, Wisconsin RID A-3395-2008. *Journal of Great Lakes Research*: **1997**, *23* (1), 61-73.

(23) Hopke, P. K. Recent Developments in Receptor Modeling. *Journal of Chemometrics*: **2003**, *17* (5), 255-265.

(24) Henry, R. C.; Christensen, E. R. Selecting an Appropriate Multivariate Source Apportionment Model Result. *Environmental Science & Technology*: **2010**, *44* (7), 2474-2481.

(25) Bzdusek, P. A.; Christensen, E. R. Comparison of a New Variant of PMF with Other Receptor Modeling Methods Using Artificial and Real Sediment PCB Data Sets. *Environmetrics*: **2006**, *17* (4), 387-403.

(26) Galarneau, E. Source Specificity and Atmospheric Processing of Airborne PAHs: Implications for Source Apportionment. *Atmospheric Environment*: **2008**, *42* (35), 8139-8149.

(27) Paatero, P.; Tapper, U. Positive Matrix Factorization: A Non-Negative Factor Model with Optimal Utilization of Error Estimates of Data Values. *Environmetrics*: **1994**, *5* (2), 111-126.

(28) Paatero, P. Least Squares Formulation of Robust Non-Negative Factor Analysis. *Chemometrics and Intelligent Laboratory Systems*: **1997**, *37* (1), 23-35.

(29) Bzdusek, P. A. *PCB or PAH Sources and Degradation in Aquatic Sediments Determined by Positive Matrix Factorization*. University of Wisconsin-Milwaukee: **2005**.

(30) USEPA EPA Positive Matrix Factorization (PMF) 3.0 Fundamentals & User Guide. *US Environmental Protection Agency, Office of Research and Development,* Washington, D.C.: **2008**.

(31) Granberg, K. J. *Multimedia Source Apportionment of Semivolatile Organic Contaminants in the Chicago Area of Influence*. University of Illinois at Chicago: **2013**.

(32) Lee, E.; Chan, C. K.; Paatero, P. Application of Positive Matrix Factorization in source Apportionment of Particulate Pollutants in Hong Kong. *Atmospheric Environment*: **1999**, *33* (19), 3201-3212.

(33) Paatero, P. User's Guide for Positive Matrix Factorization Programs PMF2 and PMF3. Part 1: Tutorial. *University of Helsinki, Helsinki, Finland*: **2003**.

(34) Soonthornnonda, P.; Zou, Y.; Christensen, E. R.; Li, A. PCBs in Great Lakes Sediments, Determined by Positive Matrix Factorization RID A-3395-2008. *Journal of Great Lakes Research*: **2011**, *37* (1), 54-63.

(35) Stout, S. A.; Emsbo-Mattingly, S. D. Concentration and Character of PAHs and Other Hydrocarbons in Coals of Varying Rank – Implications for Environmental Studies of Soils and Sediments Containing Particulate Coal. *Organic Geochemistry*: **2008**, *39* 801-819.

(36) Achten, C.; Hofmann, T. Native Polycyclic Aromatic Hydrocarbons (PAH) in Coals - A Hardly Recognized Source of Environmental Contamination. *Science of the Total Environment*: **2009**, *407* (8), 2461-2473.

(37) Chapman, P. M.; Downie, J.; Maynard, A.; Taylor, L. A. Coal and Deodorizer Residues in Marine Sediments - Contaminants or Pollutants? *Environmental Toxicology and Chemistry*: **1996**, *15* (5), 638-642.

(38) Bender, M. E.; Roberts, M. H.; DeFur, P. O. Unavailability of Polynuclear Aromatic Hydrocarbons from Coal Particles to the Eastern Oyster. *Environmental Pollution (Barking, Essex : 1987):* **1987**, *44* 243-60.

(39) Boonyatumanond, R.; Murakami, M.; Wattayakorn, G.; Togo, A.; Takada, H. Sources of Polycyclic Aromatic Hydrocarbons (PAHs) in Street Dust in a Tropical Asian Mega-City, Bangkok, Thailand. *Science of the Total Environment*: **2007**, *384* (1-3), 420-432.

(40) NIST. Certificate of Analysis, Standard Reference Material 1975. *Diesel Particulate Extract*. National Institute of Standards and Technology, Gaithersburg, MD: **2008**, pp 1-9.

(41) Laroo, C. A.; Schenk, C. R.; Sanchez, L. J.; McDonald, J. Emissions of PCDD/Fs, PCBs, and PAHs from a Modern Diesel Engine Equipped with Catalyzed Emission Control Systems. *Environmental Science & Technology*: **2011**, *45* (15), 6420-6428.

(42) Gulezian, P. Z.; Ison, J. L.; Granberg, K. J. Establishment of an Invasive Plant Species (Conium maculatum) in Contaminated Roadside Soil in Cook County, Illinois. *The American Midland Naturalist*: **2012**, *168* (2), 375-395.

(43) Wang, J.; Jia, C. R.; Wong, C. K.; Wong, P. K. Characterization of Polycyclic Aromatic Hydrocarbons Created in Lubricating Oils. *Water, Air, & Soil Pollution*: **2000**, *120* (3), 381-396.

(44) Wise, S. A.; Poster, D. L.; Leigh, S. D.; Rimmer, C. A.; Mössner, S.; Schubert, P.; Sander, L. C.; Schantz, M. M. Polycyclic Aromatic Hydrocarbons (Pahs) in a Coal Tar Standard Reference Material - SRM 1597a Updated. *Analytical and Bioanalytical Chemistry*: **2010**, *398* 717-728.

(45) Mueller, J. G.; Chapman, P. J.; Pritchard, P. H. Creosote-Contaminated Sites. Their Potential for Bioremediation. *Environmental Science & Technology*: **1989**, *23* (10), 1197-1201.

(46) Mahler, B. J.; Van Metre, P. C.; Bashara, T. J.; Wilson, J. T.; Johns, D. A. Parking Lot Sealcoat: An Unrecognized Source of Urban Polycyclic Aromatic Hydrocarbons. *Environmental Science & Technology*: **2005**, *39* (15), 5560-5566.

(47) Van Metre, P.; Mahler, B. J.; Wilson, J. T; Burbank, T. L. *Collection and Analysis of Samples for Polycyclic Aromatic Hydrocarbons in Dust and Other Solids Related to Sealed and Unsealed Pavement from 10 Cities Across the United States, 2005-07*. US Department of the Interior, US Geological Survey, Data Series 361: **2008**.

(48) Boonyatumanond, R.; Wattayakorn, G.; Togo, A.; Takada, H. Distribution and Origins of Polycyclic Aromatic Hydrocarbons (PAHs) in Riverine, Estuarine, and Marine Sediments in Thailand. *Marine Pollution Bulletin*: **2006**, *52* 942-56.

(49) NIST. Certificate of Analysis, Standard Reference Material 1649b. Urban Dust. *National Institute of Standards and Technology*, Gaithersburg, MD: **2009**, 1-14.

(50) Stout, S. A.; Emsbo-Mattingly, S. D. Concentration and Character of PAHs and Other Hydrocarbons in Coals of Varying Rank - Implications for Environmental Studies of Soils and Sediments Containing Particulate Coal. *Organic Geochemistry*: **2008**, *39* (7), 801-819.

(51) Van Metre, P. C.; Mahler, B. J. Contribution of PAHs from Coal-Tar Pavement Sealcoat and Other Sources to 40 U.S. Lakes. *The Science of the Total Environment*: **2010**, *409* 334-44.

(52) Christensen, E. R.; Arora, S. Source Apportionment of PAHs in Sediments Using Factor Analysis by Time Records: Application to Lake Michigan, USA. *Water Research*: **2007**, *41* (1), 168-176.